

## Collisional picture of quantum optics with giant emitters

Dario Cilluffo <sup>1,2</sup> Angelo Carollo <sup>1,3</sup> Salvatore Lorenzo,<sup>1</sup> Jonathan A. Gross <sup>4</sup>  
G. Massimo Palma <sup>1,2</sup> and Francesco Ciccarello <sup>1,2</sup>

<sup>1</sup>*Dipartimento di Fisica e Chimica “Emilio Segrè,” Università degli Studi di Palermo, Via Archirafi 36, 90123 Palermo, Italy*

<sup>2</sup>*NEST, Istituto Nanoscienze CNR, Piazza S. Silvestro 12, 56127 Pisa, Italy*

<sup>3</sup>*Radiophysics Department, National Research Lobachevsky State University of Nizhni Novgorod, 23 Gagarin Avenue, Nizhni Novgorod 603950, Russia*

<sup>4</sup>*Institut Quantique, Université de Sherbrooke, Sherbrooke, Quebec, Canada J1K 2R1*



(Received 22 June 2020; accepted 23 August 2020; published 13 October 2020)

The effective description of the weak interaction between an emitter and a bosonic field as a sequence of two-body collisions provides a simple intuitive picture compared to traditional quantum optics methods as well as an effective calculation tool of the joint emitter-field dynamics. Here this collisional approach is extended to many emitters (atoms or resonators), each generally interacting with the field at many coupling points (giant emitter). In the regime of negligible delays, the unitary describing each collision in particular features a contribution of a chiral origin resulting in an effective Hamiltonian. The picture is applied to derive a Lindblad master equation (ME) of a set of giant atoms coupled to a (generally chiral) waveguide field in an arbitrary white-noise Gaussian state, which condenses into a single equation and extends a variety of quantum optics and waveguide QED MEs. The effective Hamiltonian and jump operators corresponding to a selected photodetection scheme are also worked out.

DOI: [10.1103/PhysRevResearch.2.043070](https://doi.org/10.1103/PhysRevResearch.2.043070)

## I. INTRODUCTION

A major focus of quantum optics is the interaction of quantum emitters, such as (artificial) atoms or resonators, with a field modeled as a continuum of bosonic modes. Accordingly, describing the dynamics generally requires keeping track of all the field modes, a task which at times can be circumvented when the focus is the open dynamics of the emitters, provided a master equation is preliminarily derived and ensured to be completely positive. This tool is yet insufficient and must be complemented with appropriate field equations whenever one is interested in the dynamics of photons.

A somewhat unconventional method to tackle quantum optics problems is a collision-model description, an approach adopted in a growing number of works [1–15]. Much like in standard theories of photon counting statistics, the basic idea (see Fig. 1) is decomposing the field into discrete time bins (each with an associated bosonic mode). In the interaction picture, time bins travel at constant speed so as to collide one at a time with the quantum emitter (conveyor-belt-like dynamics). This reduces the complex emitter-field interaction to a sequence of elementary two-body collisions, each involving a different time bin: a dynamics known in some

literature as the collision model (CM) or repeated interactions model. Collision models are being routinely used in various areas such as weak continuous measurements [16,17], non-Markovian quantum dynamics [18–28], quantum thermodynamics [29–34], and even quantum gravity [35,36].

The CM-based description has a number of interesting features such as (i) a simple and intuitive picture of the joint dynamics, which is helpful to get insight into the problem at hand; (ii) a direct Born-Markov-approximation-free derivation of Lindblad master equations (MEs) guaranteed to be completely positive; (iii) the time-bin evolution being easily worked out, thus enabling one to keep track of a relevant part of the field dynamics; (iv) CMs being the natural microscopic framework to describe continuous weak measurements, which can be applied to photon detection [8,16,17,36]; and (v) when formulated as a CM, the dynamics turns into an equivalent quantum circuit, allowing in particular for matrix product state simulations [1,8,11,37–39].

In the framework of quantum optics, so far only CMs for pointlike quantum emitters have been fully developed (only one coupling point). While CMs featuring two coupling points were considered in the regime of long time delays [1,2,5], a comprehensive formulation of the negligible-delay regime (occurring in most experiments) is still missing.

In this work we present a general theory of the CM-based description of quantum optics in the case of many emitters. We allow each of these to generally couple to the field at many coupling points so as to encompass systems such as the so-called giant atoms [40,41], which can now be experimentally implemented and operated [42,43], or bosonic oscillators/atomic ensembles coupled to one-dimensional

---

Published by the American Physical Society under the terms of the [Creative Commons Attribution 4.0 International](https://creativecommons.org/licenses/by/4.0/) license. Further distribution of this work must maintain attribution to the author(s) and the published article's title, journal citation, and DOI.

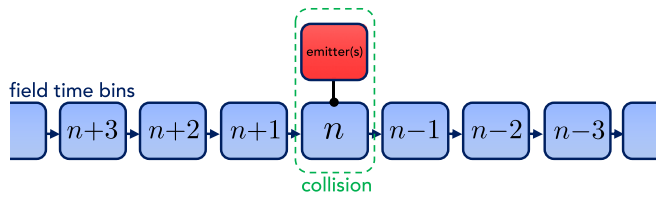


FIG. 1. Basic collision-model description of the emitter-field dynamics. The field is decomposed into noninteracting time bins traveling at constant speed. One at a time, these undergo a short two-body interaction with the emitter (collision). In the regime of negligible time delays, a similar conveyor-belt picture holds for many emitters, each of which can be giant (i.e., interacting with the field at many coupling points).

fields in looped geometries [44,45] as explicitly discussed in Ref. [46]. The framework is first formulated by considering a unidirectional field (just like in the standard input-output formalism [47]) and then extended to a bidirectional field. While the regimes of both negligible and long time delays are discussed, our main focus is the former. In this case it will be proven that each collision can be effectively represented as a collective coupling of all the emitters with one field time bin plus an internal coherent dipole-dipole interaction between the emitters described by a Hamiltonian originating from the intrinsic system's chirality (in the conveyor-belt picture of Fig. 1 time bins travel from left to right).

While the presented collisional framework has many potential uses, here we apply it to derive the Lindblad master equation of a set of giant emitters coupled to a, generally chiral, one-dimensional waveguide when the field starts in an arbitrary Gaussian state. This condenses in a single equation and extends a variety of master equations used in waveguide QED [40,48–50], as will be illustrated in detail. Moreover, we show that the recently discovered possibility to realize decoherence-free Hamiltonians with giant emitters [46,51] is naturally predicted in the collisional picture, without the need to resort to the master equation, thus highlighting its independence of the field state. Additionally, for an arbitrary photodetection scheme, we calculate the Kraus operators corresponding to a measurement outcome and use these to derive the effective Hamiltonian and jump operators generating the quantum trajectories.

The present paper in fact comprises two parts. The first presents the general emitter-field microscopic model (Sec. II) and outlines the main collision-model features without proof, the aforementioned general master equation, and the description of photodetection and related quantum trajectories (Sec. III). Special cases of the master equation are illustrated in a separate section (Sec. IV), which ends with a discussion of decoherence-free Hamiltonians (Sec. IV).

The second (more technical) part derives in detail the collision model for a unidirectional field (Sec. V), works out the ensuing master equation (when existing) in the negligible-delay regime (Sec. VI), extends these tasks to a bidirectional field (Secs. VII and VIII), and finally addresses in detail photodetection and quantum trajectories (Sec. IX).

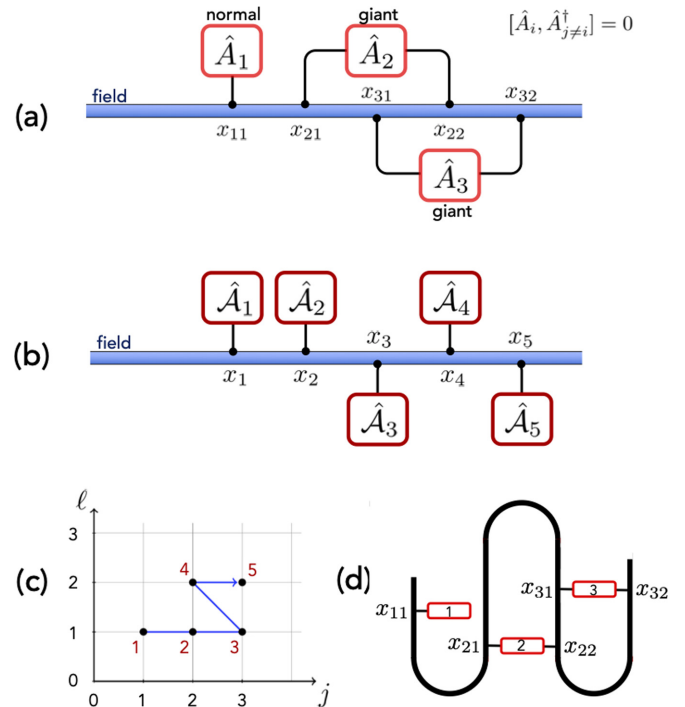


FIG. 2. Set of (generally giant) emitters coupled to a unidirectional field. (a) A normal emitter (such as 1) interacts with the field at a single coupling point, while a giant emitter has two or more coupling points (like emitters 2 and 3 here). (b) Instead of a double index as in (a), we can use a single index  $\nu$  to label coupling points from left to right, defining for each a ladder operator  $\hat{A}_\nu$ , incorporating the coordinate-dependent phase factor (e.g.,  $\hat{A}_4 = e^{-ik_0 x_{22}} \hat{A}_2$ ). Thus, formally, the system is equivalent to a set of normal but *not* independent emitters, i.e.,  $[\hat{A}_\nu, \hat{A}_{\nu'}^\dagger]$  for  $\nu \neq \nu'$  is generally nonzero (e.g.,  $[\hat{A}_1, \hat{A}_2^\dagger] = e^{ik_0(x_{21}-x_{11})}[\hat{A}_1, \hat{A}_2^\dagger] = 0$  but  $[\hat{A}_2, \hat{A}_4^\dagger] = e^{ik_0(x_{22}-x_{21})}[\hat{A}_2, \hat{A}_4^\dagger] \neq 0$ ). (c) Transformation from indexing (b) to (a) is described by the pair of index functions  $j = \mathcal{J}_\nu$  and  $\ell = \mathcal{L}_\nu$ . These and the inverse function can be represented through the plotted diagram, where values of  $\nu$  (in red) label the black dots. The Cartesian coordinates of each dot indicate the corresponding pair  $(j, \ell)$ . The diagram thus encodes the coupling points topology. (d) Implementation of the setup in (a) via a looped unidirectional waveguide.

## II. MICROSCOPIC MODEL

The general emitter-field microscopic model we consider is essentially the same as that underpinning the standard input-output formalism of quantum optics [47] and related theories such as the SLH framework [52].

Let  $S$  be a system made out of  $N_e$  quantum emitters of frequency  $\omega_0$  and associated ladder operators  $\hat{A}_j$  and  $\hat{A}_j^\dagger$  for  $j = 1, \dots, N_e$ . The statistical nature of these operators is left unspecified; hence, in particular, each emitter could be a harmonic oscillator or a pseudospin (linear and nonlinear, respectively). The emitters are weakly coupled to a unidirectional bosonic field with normal-mode ladder operators  $\hat{b}_\omega$  and  $\hat{b}_\omega^\dagger$  such that  $[\hat{b}_\omega, \hat{b}_{\omega'}] = [\hat{b}_\omega^\dagger, \hat{b}_{\omega'}^\dagger] = 0$  and  $[\hat{b}_\omega, \hat{b}_{\omega'}^\dagger] = \delta(\omega - \omega')$ . The  $j$ th emitter interacts with the field at  $\mathcal{N}_j$  distinct coupling points. For  $\mathcal{N}_j = 1$  we retrieve the standard local coupling and the emitter is called normal [see Fig. 2(a)].

Instead, if  $\mathcal{N}_j \geq 2$ , the coupling is multilocal and the emitter is dubbed giant [see Figs. 2(a) and 2(d)]. The spatial coordinate of the  $\ell$ th coupling point of the  $j$ th emitter is  $x_{j\ell}$  (the field is along the  $x$  axis). Under the usual rotating-wave approximation (RWA) and assuming white coupling, the total Hamiltonian reads (we set  $\hbar = 1$ )

$$\hat{H} = \hat{H}_S + \hat{H}_f + \hat{V}, \quad (1)$$

where

$$\hat{H}_S = \sum_{j=1}^{N_e} \omega_0 \hat{A}_j^\dagger \hat{A}_j, \quad \hat{H}_f = \int d\omega (\omega_0 + \omega) \hat{b}_\omega^\dagger \hat{b}_\omega, \quad (2)$$

$$\hat{V} = \sum_{j=1}^{N_e} \sum_{\ell=1}^{\mathcal{N}_j} \sqrt{\frac{\gamma}{2\pi}} e^{i\omega_0 \tau_{j\ell}} \int d\omega e^{i\omega \tau_{j\ell}} \hat{A}_j^\dagger \hat{b}_\omega + \text{H.c.}, \quad (3)$$

with all integrals running over the entire real axis compatibly with the RWA. Here  $\tau_{j\ell} = x_{j\ell}/v$  is the coordinate in the time domain of each coupling point (the field dispersion law is  $\omega = vk$ ). Note that here  $\omega$  are frequencies measured from the emitters' energy  $\omega_0$  (i.e., detunings in fact). We also point out that each coupling point has an associated position-dependent phase factor  $e^{i\omega_0 \tau_{j\ell}}$ , which can be equally written in the space domain as  $e^{ik_0 x_{j\ell}}$ , with  $k_0 = \omega_0/v$ . Instead of  $\omega$ -dependent normal modes, the field can be equivalently represented in terms of time modes with ladder operators

$$\hat{b}_t = \frac{1}{\sqrt{2\pi}} \int d\omega \hat{b}_\omega e^{-i\omega t}, \quad (4)$$

fulfilling bosonic commutation rules

$$[\hat{b}_t, \hat{b}_{t'}^\dagger] = \delta(t - t'), \quad [\hat{b}_t, \hat{b}_{t'}] = [\hat{b}_t^\dagger, \hat{b}_{t'}^\dagger] = 0. \quad (5)$$

### A. Interaction picture and relabeling

Passing to the interaction picture with respect to  $\hat{H}_0 = \hat{H}_S + \hat{H}_f$  transforms ladder operators as  $\hat{A}_j \rightarrow \hat{A}_j e^{-i\omega_0 t}$  and  $\hat{b}_\omega \rightarrow \hat{b}_\omega e^{-i(\omega_0 + \omega)t}$  so that the joint emitter-field state  $\sigma$  now evolves as  $\dot{\sigma} = -i[\hat{V}_t, \sigma]$ , with

$$\hat{V}_t = \sqrt{\gamma} \sum_{j,\ell} \hat{A}_j^\dagger e^{i\omega_0 \tau_{j\ell}} \hat{b}_{t-\tau_{j\ell}} + \text{H.c.} \quad (6)$$

Now, following Ref. [46], it is convenient to introduce an index  $\nu = 1, \dots, \mathcal{N}$  labeling all the coupling points from left to right, i.e.,  $x_1 < x_2 < \dots < x_{\mathcal{N}}$  [see Fig. 2(b)] or equivalently in the time domain  $\tau_1 < \tau_2 < \dots < \tau_{\mathcal{N}}$  (here  $\mathcal{N} = \sum_{j=1}^{N_e} \mathcal{N}_j$  is the total number of coupling points). For each coupling point  $\nu$ , we define a corresponding ladder operator as

$$\hat{A}_\nu = \hat{A}_j e^{-ik_0 x_{j\ell}}, \quad (7)$$

with  $\hat{A}_j$  the ladder operator of the corresponding atom and  $e^{-ik_0 x_{j\ell}}$  the corresponding phase shift. For instance, in the case of Fig. 2(a),  $\mathcal{A}_5 = \hat{A}_3 e^{-ik_0 x_{32}} = \hat{A}_3 e^{-i\omega_0 \tau_{32}}$ . Formally, the mapping between  $(j, \ell)$  and  $\nu$  is expressed by a pair of discrete functions  $j = \mathcal{J}_\nu$  and  $\ell = \mathcal{L}_\nu$ , a diagrammatic representation of which is shown in Fig. 2(c). Note that ladder operators  $\{\hat{A}_\nu\}$  with different indices do not necessarily commute, that is,  $[\hat{A}_\nu, \hat{A}_{\nu' \neq \nu}^\dagger]$  is generally nonzero [e.g., in Fig. 2(b),  $[\mathcal{A}_1, \mathcal{A}_3^\dagger] = 0$  but  $[\mathcal{A}_3, \mathcal{A}_5^\dagger] \neq 0$ ]. In this way the system could

be thought of as a set of  $\mathcal{N}$  normal emitters (as many as the coupling points), which yet are not independent. Their dynamics is governed by the Hamiltonian [cf. Eq. (6)]

$$\hat{V}_t = \sqrt{\gamma} \sum_{\nu=1}^{\mathcal{N}} \hat{A}_\nu^\dagger \hat{b}_{t-\tau_\nu} + \text{H.c.} \quad (8)$$

### B. Bidirectional field

For a bidirectional field, each normal frequency  $\omega$  now has associated right-going and left-going modes with ladder operators  $\hat{b}_\omega$  and  $\hat{b}'_\omega$ , respectively ( $\hat{b}'_\omega$  fulfills commutation rules analogously to  $\hat{b}_\omega$ ). In the total Hamiltonian (1), the field and coupling Hamiltonians are replaced by

$$\hat{H}_f = \int d\omega (\omega_0 + \omega) (\hat{b}_\omega^\dagger \hat{b}_\omega + \hat{b}'_\omega \hat{b}'_\omega), \quad (9)$$

$$\begin{aligned} \hat{V} = & \sqrt{\frac{\gamma}{2\pi}} \sum_{j,\ell} e^{i\omega_0 \tau_{j\ell}} \int d\omega e^{i\omega \tau_{j\ell}} \hat{A}_j^\dagger \hat{b}_\omega \\ & + \sqrt{\frac{\gamma'}{2\pi}} \sum_{j,\ell} e^{-i\omega_0 \tau_{j\ell}} \int d\omega e^{i\omega \tau_{j\ell}} \hat{A}_j^\dagger \hat{b}'_\omega + \text{H.c.}, \end{aligned} \quad (10)$$

where we allowed generally different coupling strengths to right- and left-going modes so as to encompass chiral dynamics [53] (the previous unidirectional case is retrieved for  $\gamma' = 0$ ). Note the different phase factors in right-going terms compared to left-going ones. A detailed derivation of the microscopic Hamiltonian is reviewed in Appendix A.

Left-going time modes are defined analogously to (4) as

$$\hat{b}'_t = \frac{1}{\sqrt{2\pi}} \int d\omega \hat{b}'_\omega e^{-i\omega t}, \quad (11)$$

fulfilling commutation rules analogously to (5). Proceeding similarly to the unidirectional case leads to the interaction-picture coupling Hamiltonian [cf. Eq. (8)]

$$\hat{V}_t = \sqrt{\gamma} \sum_{\nu=1}^{\mathcal{N}} \hat{A}_\nu^\dagger \hat{b}_{t-\tau_\nu} + \sqrt{\gamma'} \sum_{\nu=1}^{\mathcal{N}} \hat{A}_\nu^\dagger \hat{b}'_{t+\tau_\nu} + \text{H.c.}, \quad (12)$$

with  $\hat{A}_\nu$  defined as in Eq. (7) and

$$\hat{A}'_\nu = \hat{A}_j e^{ik_0 x_{j\ell}}, \quad (13)$$

where, just like in Eq. (13),  $j = \mathcal{J}_\nu$  and  $\ell = \mathcal{L}_\nu$  (note however the change of phase compared to  $\hat{A}_\nu$ ).

## III. SUMMARY OF MAIN RESULTS

In this section we sum up some of the main results of this work.

### A. Unidirectional field

Let  $t_n = n\Delta t$ , with  $n$  an integer and  $t_0$  the initial time, be a mesh of the time axis. In the regime of negligible time delays defined by  $t_{\mathcal{N}} - t_1 \ll \Delta t \ll \gamma^{-1}$  [see Fig. 3(a)], the propagator of the joint dynamics (in the interaction picture) is well approximated as

$$\hat{U}_t \simeq \prod_{n=1}^{\lfloor t/\Delta t \rfloor} \hat{U}_n, \quad (14)$$

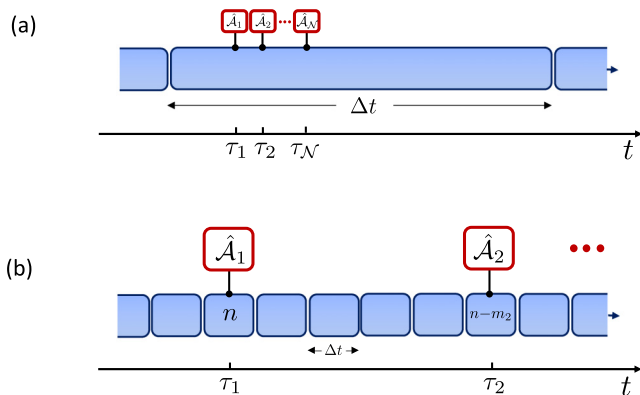


FIG. 3. Effective collision model for a unidirectional field in the regimes of (a) negligible and (b) non-negligible time delays. (a) Negligible time delays  $\tau_v - \tau_{v-1} \ll \Delta t \ll \gamma^{-1}$  for any  $v$ . The time bin is much larger than the distance (in the time domain) between coupling points. Note, though, that so long as time delays are finite (no matter how short) the behavior is different from the ideal case of colocated coupling points; the fact that each time bin collides first with  $v = 1$ , then  $v = 2$ , etc., produces the effective Hamiltonian (15). (b) Non-negligible time delays  $\Delta t \ll \tau_v - \tau_{v-1} \ll \gamma^{-1}$  for any  $v$ . Distinct coupling points collide with different, generally nonconsecutive, time bins.

with  $\hat{U}_n = e^{-i(\hat{H}_{\text{vac}} + \hat{V}_n)\Delta t}$ , where

$$\hat{H}_{\text{vac}} = i\frac{\gamma}{2} \sum_{v>v'} (\hat{A}_v^\dagger \hat{A}_{v'} - \hat{A}_{v'}^\dagger \hat{A}_v), \quad (15)$$

$$\hat{V}_n = \sqrt{\frac{\gamma}{\Delta t}} (\hat{A}^\dagger \hat{b}_n + \text{H.c.}) \quad (16)$$

(note the characteristic  $1/\sqrt{\Delta t}$  dependence of the coupling strength). Here  $\hat{A}$  is the collective emitters' operator  $\hat{A} = \sum_v \hat{A}_v$ , while

$$\hat{b}_n = \frac{1}{\sqrt{\Delta t}} \int_{t_{n-1}}^{t_n} dt \hat{b}_t \quad (17)$$

is the annihilation operator associated with the  $n$ th time bin of the field. Time-bin ladder operators fulfill standard bosonic commutation rules  $[\hat{b}_n, \hat{b}_{n'}] = [\hat{b}_n^\dagger, \hat{b}_{n'}^\dagger] = 0$  and  $[\hat{b}_n, \hat{b}_{n'}^\dagger] = \delta_{n,n'}$ .

Thus the dynamics effectively consists of a sequence of pairwise collisions (short interactions). During the  $n$ th collision, the emitters collectively couple to the  $n$ th field's time bin (interaction  $\hat{V}_n$ ) and at the same time undergo an effective dipole-dipole interaction described by the Hamiltonian  $\hat{H}_{\text{vac}}$ . Note that time bins are noninteracting with each other and that the  $n$ th time bin interacts with the emitters only during the time interval  $[t_{n-1}, t_n]$  in a conveyor-belt fashion, in this respect just like the standard case of one normal emitter (see Fig. 1). Note that the dipole-dipole Hamiltonian (15) has a chiral origin: It arises because each time bin (see Fig. 1) collides *first* with coupling point  $v = 1$ , then  $v = 2$ , and so on. Indeed if all the coupling points had the same location,  $\hat{V}_n$  would still be present but  $\hat{H}_{\text{vac}} = 0$ .

Let  $\sigma_n = \sigma_{t=t_n}$  be the joint state of the emitters and all time bins with  $\sigma_0 = \rho_0 \otimes \rho_f$ , where  $\rho_0$  ( $\rho_f$ ) is the initial state of

emitters (field). At each collision,  $\sigma_n$  evolves according to

$$\frac{\Delta \sigma_n}{\Delta t} = -i[\hat{H}_{\text{vac}} + \hat{V}_n, \sigma_{n-1}] + \Delta t (\hat{V}_n \sigma_{n-1} \hat{V}_n - \frac{1}{2} [\hat{V}_n^2, \sigma_{n-1}]_+), \quad (18)$$

where  $\Delta \sigma_n = \sigma_n - \sigma_{n-1}$  and  $[\dots]_+$  stands for the anti-commutator (the  $\Delta t$  dependence of second-order terms is only apparent since  $\hat{V}_n \sim 1/\sqrt{\Delta t}$ ). If the initial state of the time bins corresponding to the field state  $\rho_f$  is of the form  $\bigotimes_n \eta_n$  (no correlations), then tracing off the field in Eq. (18) yields that the emitters undergo a Markovian dynamics described by

$$\frac{\Delta \rho_n}{\Delta t} = -i[\hat{H}_{\text{vac}} + \langle \hat{V}_n \rangle, \rho_{n-1}] + \Delta t \text{Tr}_n \{ \hat{V}_n \rho_{n-1} \hat{V}_n - \frac{1}{2} [\hat{V}_n^2, \rho_{n-1} \eta_n]_+ \}, \quad (19)$$

with  $\rho_n$  the state of the emitters at time  $t_n$ ,  $\Delta \rho_n = \rho_n - \rho_{n-1}$ , and  $\langle \dots \rangle = \text{Tr}_n \{ \dots \eta_n \}$ , where  $\text{Tr}_n \{ \dots \}$  is the partial trace over time bin  $n$ . Equation (19) can always be expressed in the standard Lindblad form  $\Delta \rho_n / \Delta t = -i[\hat{\mathcal{H}}, \rho_{n-1}] + \sum_m \mathcal{D}_{\hat{J}_m}[\rho_{n-1}]$ , with  $\hat{\mathcal{H}} = \hat{H}_{\text{vac}}$  and

$$\mathcal{D}_{\hat{J}}[\rho] = \hat{J} \rho \hat{J}^\dagger - \frac{1}{2} [\hat{J}^\dagger \hat{J}, \rho]_+, \quad (20)$$

where  $\{\hat{J}_m\}$  is a suitable collection of jump operators. The Lindblad form is guaranteed because at each collision the emitters evolve according to a completely positive and trace-preserving (CPTP) map  $\rho_n = \langle \hat{U}_n \rho_{n-1} \hat{U}_n^\dagger \rangle$ .

The most general white-noise Gaussian state of the field is fully specified by the first and second moments [54]

$$\langle d\hat{b}_t \rangle = \alpha_t dt, \quad \langle d\hat{b}_t^\dagger d\hat{b}_t \rangle = N dt, \quad \langle d\hat{b}_t d\hat{b}_t \rangle = M dt, \quad (21)$$

with  $d\hat{b}_t = \int_t^{t+dt} ds \hat{b}_s$  the well-known quantum noise increment. Correspondingly, the most general Gaussian uncorrelated state of the time bins is fully specified by the moments

$$\langle \hat{b}_n \rangle = \alpha_n \sqrt{\Delta t}, \quad \langle \hat{b}_n^\dagger \hat{b}_{n'} \rangle = \delta_{n,n'} N, \quad \langle \hat{b}_n \hat{b}_{n'} \rangle = \delta_{n,n'} M, \quad (22)$$

with  $\alpha_n = \alpha_{t=t_n}$ ,  $N \geq 0$ , and  $|M|^2 \leq N(N+1)$ .

Replacing the explicit expression of  $\hat{V}_n$  in Eq. (19) using (22) and carrying out the continuous-time limit  $\gamma \Delta t \rightarrow 0$ , the discrete master equation (19) is turned into the general continuous-time master equation

$$\frac{d\rho}{dt} = -i[\hat{H}_{\text{vac}} + \sqrt{\gamma}(\alpha_t^* \hat{A} + \text{H.c.}), \rho] + \gamma(N+1) \mathcal{D}_{\hat{A}}[\rho] + \gamma N \mathcal{D}_{\hat{A}^\dagger}[\rho] + \gamma \{ M(\hat{A}^\dagger \rho \hat{A}^\dagger - \frac{1}{2} [\hat{A}^{\dagger 2}, \rho]_+) + \text{H.c.} \}. \quad (23)$$

This can be expressed in terms of original ladder operators  $\hat{A}_j$  using (7) and recalling  $\hat{A} = \sum_v \hat{A}_v$ .

## B. Bidirectional field

In the case of a bidirectional field, the time bin is now bipartite (see Fig. 4) having associated ladder operators  $\hat{b}_n$  [cf. Eq. (17)] and  $\hat{b}'_n$ , the latter given by

$$\hat{b}'_n = \frac{1}{\sqrt{\Delta t}} \int_{t_{n-1}}^{t_n} dt \hat{b}'_t, \quad (24)$$

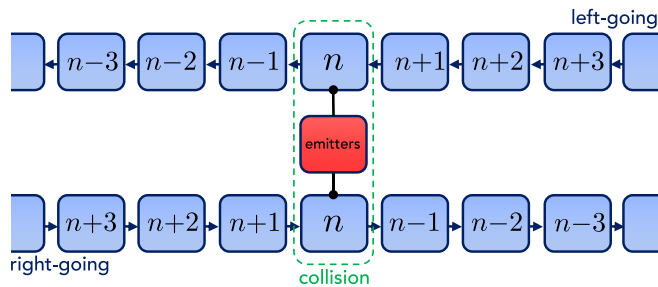


FIG. 4. Collision-model description for a bidirectional field. Each time bin is now bipartite, comprising a right-going mode (bottom) and a left-going mode (top). At each collision the emitters jointly collide with the two-mode time bin according to the coupling Hamiltonian (26) and additionally are subject to an internal coherent dynamics corresponding to the dipole-dipole Hamiltonian (25).

while  $\hat{H}_{\text{vac}}$  and  $\hat{V}_n$  are now generalized as

$$\hat{H}_{\text{vac}} = \frac{i}{2} \sum_{v>v'} (\gamma \hat{A}_v^\dagger \hat{A}_v + \gamma' \hat{A}_v'^\dagger \hat{A}_v' - \text{H.c.}), \quad (25)$$

$$\hat{V}_n = \frac{1}{\sqrt{\Delta t}} (\sqrt{\gamma} \hat{A}^\dagger \hat{b}_n + \sqrt{\gamma'} \hat{A}'^\dagger \hat{b}'_n + \text{H.c.}), \quad (26)$$

with

$$\hat{A} = \sum_v \hat{A}_v, \quad \hat{A}' = \sum_v \hat{A}'_v. \quad (27)$$

Inside parentheses in (25), note that the second term has swapped subscripts compared to the first. This is due to the opposite interaction time ordering for left- and right-going modes.

Accordingly, the dissipator in the Lindblad master equation (23) now naturally splits into a pair of analogous contributions: one featuring operators  $\hat{A}_v$  and moments of right-going field modes ( $\alpha_r$ ,  $N$ , and  $M$ ) and another one involving  $\hat{A}'_v$  and left-going-mode moments ( $\alpha'_l$ ,  $N'$ , and  $M'$ ). The latter moments are defined analogously to (21) with  $\hat{b}_l \rightarrow \hat{b}'_l$ . This leads to the master equation

$$\begin{aligned} \frac{d\rho}{dt} = & -i[\hat{H}_{\text{vac}} + \sqrt{\gamma}(\alpha_r^* \hat{A} + \alpha_r \hat{A}^\dagger + \text{H.c.}), \rho] \\ & + \gamma(N+1)\mathcal{D}_{\hat{A}}[\rho] + \gamma N \mathcal{D}_{\hat{A}^\dagger}[\rho] \\ & + \gamma'(N'+1)\mathcal{D}_{\hat{A}'}[\rho] + \gamma' N' \mathcal{D}_{\hat{A}'^\dagger}[\rho] \\ & + \gamma \{M(\hat{A}^\dagger \rho \hat{A}^\dagger - \frac{1}{2}[\hat{A}^{\dagger 2}, \rho]_+) + \text{H.c.}\} \\ & + \gamma' \{M'(\hat{A}'^\dagger \rho \hat{A}'^\dagger - \frac{1}{2}[\hat{A}'^{\dagger 2}, \rho]_+) + \text{H.c.}\}. \end{aligned} \quad (28)$$

where we recall Eqs. (20) and (25). This can be expressed in terms of original ladder operators  $\hat{A}_j$  through (7), (13), and (27). The master equation (23) for a unidirectional field is retrieved for  $\gamma' = 0$ .

### C. Photodetection and quantum trajectories

For a unidirectional field, photodetection translates into measuring each time bin right after its collision with  $S$  in a selected basis  $\{|k\rangle_n\}$  (defining the photodetection scheme). For time bins initially in state  $\bigotimes_n |\chi_n\rangle$  (thus  $\eta_n = |\chi_n\rangle\langle\chi_n|$ ) and negligible time delays, the (unnormalized) state of  $S$  after a

specific sequence of measurement outcomes  $\{k_1, \dots, k_n\}$  is

$$\tilde{\rho}_n = \hat{K}_{k_n} \dots \hat{K}_{k_1} \rho_0 \hat{K}_{k_1}^\dagger \dots \hat{K}_{k_n}^\dagger, \quad (29)$$

the associated probability being  $p_{k_1 \dots k_n} = \text{Tr}_S\{\tilde{\rho}_n\}$  and with each Kraus operator given by

$$\hat{K}_{k_m} = \langle k_m | \hat{U}_m | \chi_m \rangle. \quad (30)$$

A measurement on time bin  $n$  with outcome  $k$  (at the end of the  $n$ th collision) thus projects  $S$  into the (unnormalized) state  $\tilde{\rho}_n = \hat{K}_k \rho_{n-1} \hat{K}_k^\dagger$  with probability  $p_k = \text{Tr}_S\{\tilde{\rho}_n\}$ , defining the conditional dynamics. Summing over all possible outcomes yields the CPTP map  $\rho_n = \mathcal{E}[\rho_{n-1}] = \sum_k \hat{K}_k \rho_{n-1} \hat{K}_k^\dagger$ , defining the unconditional dynamics.

A (pure) time-bin state generally depends itself on  $\sqrt{\Delta t}$ . We consider those states that to the lowest order in  $\sqrt{\Delta t}$  read

$$|\chi_n\rangle \simeq |0_n\rangle + |\chi_n^{(1)}\rangle \sqrt{\Delta t} + |\chi_n^{(2)}\rangle \Delta t, \quad (31)$$

with  $|\chi_n^{(j)}\rangle$  such that  $\langle \chi_n | \chi_n \rangle = 1 + O(\Delta t)$  ( $|\kappa_n\rangle$ , with  $\kappa_n = 0, 1, \dots$ , denotes the time-bin Fock states). Plugging this and  $\hat{U}_n = e^{-i(\hat{H}_{\text{vac}} + \hat{V}_n)}$  into  $\rho_n = \mathcal{E}[\rho_{n-1}]$  and dropping high-order terms eventually leads to the master equation

$$\frac{\Delta \rho_n}{\Delta t} = -i[\hat{H}_{\text{eff}}, \rho_{n-1}] + \sum_k \mathcal{D}_{\hat{J}_k}[\rho_{n-1}], \quad (32)$$

with the effective Hamiltonian  $\hat{H}_{\text{eff}}$  and jump operators  $\hat{J}_k$  given by

$$\hat{H}_{\text{eff}} = \hat{H}_{\text{vac}} + (\frac{1}{2} \sqrt{\gamma} \langle 0_n | \hat{b}_n | \chi_n^{(1)} \rangle \hat{A}^\dagger + \text{H.c.}), \quad (33)$$

$$\hat{J}_k = \langle k_n | \chi_n^{(1)} \rangle - i \sqrt{\gamma} \langle k_n | 1_n \rangle \hat{A}. \quad (34)$$

This in fact defines an unraveling of master equation (23) [which is indeed equivalent to (32)] corresponding to the photodetection scheme  $\{|k_n\rangle\}$  in the case of a unidirectional field.

For a coherent-state wave packet of amplitude  $\xi_t$  (in the time domain),<sup>1</sup>  $|\xi\rangle = \exp[\int dt (\xi_t \hat{b}_t^\dagger - \xi_t^* \hat{b}_t)] |0\rangle$  (with  $|0\rangle$  the field vacuum), the corresponding time-bin state is

$$|\chi_n\rangle = e^{\xi_n \sqrt{\Delta t} \hat{b}_n^\dagger - \xi_n^* \sqrt{\Delta t} \hat{b}_n} |0_n\rangle, \quad (35)$$

with  $\xi_n = \xi_{t=t_n}$ . Hence,  $|\chi_n^{(1)}\rangle = \xi_n |1_n\rangle$ . In the case of photon counting,  $\{|k_n\rangle\}$  are the Fock states. The effective Hamiltonian and the only surviving jump operator are thus immediately calculated as

$$\hat{H}_{\text{eff}} = \hat{H}_{\text{vac}} + \frac{1}{2} \sqrt{\gamma} (\xi_n \hat{A}^\dagger + \text{H.c.}), \quad \hat{J}_1 = \xi_n - i \sqrt{\gamma} \hat{A}. \quad (36)$$

The continuous-time limit expressions are simply obtained by replacing  $\xi_n \rightarrow \xi_t$ .

For a bidirectional field, photodetection consists in measuring both the right- and left-going time bins (see Fig. 4) in a basis  $|k, k'\rangle$ . A measurement outcome  $k, k'$  is now described by the Kraus operator [cf. Eq. (30)]

$$\hat{K}_{k,k'} = \langle k, k' | \hat{U}_m | \chi_m, \chi'_m \rangle, \quad (37)$$

<sup>1</sup>Note that  $\hat{b}_t$  [cf. Eq. (4)] are defined in terms of  $\omega$  measured from  $\omega_0$ . Thus,  $\xi_t$  specifies the wave packet in a frame rotating at frequency  $\omega_0$ .

with  $|\chi_m\rangle$  ( $|\chi'_m\rangle$ ) the initial state of the right-going (left-going) time bin and  $\hat{U}_n = e^{-i(\hat{H}_{\text{vac}} + \hat{V}_n)}$ , with  $\hat{H}_{\text{vac}}$  and  $\hat{V}_n$  now given by (25) and (26).

The effective Hamiltonian and jump operators are given by [cf. Eqs. (33) and (34)]

$$\hat{H}_{\text{eff}} = \hat{H}_{\text{vac}} + \frac{1}{2}(\sqrt{\gamma'} \langle 0 | \hat{b}_n | \chi^{(1)} \rangle \hat{A}^\dagger + \sqrt{\gamma'} \langle 0 | \hat{b}'_n | \chi'^{(1)} \rangle \hat{A}^\dagger), \quad (38)$$

$$\hat{J}_{k,k'} = \langle k|0\rangle \langle k' | \chi^{(1)} \rangle + \langle k'|0\rangle \langle k | \chi^{(1)} \rangle - i(\sqrt{\gamma'} \langle k'|0\rangle \langle k | 1 \rangle \hat{A} + \sqrt{\gamma'} \langle k|0\rangle \langle k' | 1 \rangle \hat{A}'). \quad (39)$$

Note that the unraveling defined by  $\hat{H}_{\text{eff}}$  and  $\hat{J}_{k,k'}$  can also be exploited as an effective recipe to numerically solve the master equation (28) especially when  $N_e$  is large, which generalizes to giant emitters quantum-jump methods employed for normal emitters (see, e.g., Refs. [38,55]).

#### IV. EXAMPLES OF MASTER EQUATIONS AND DECOHERENCE-FREE HAMILTONIANS

The aim of this section is to illustrate how (28) encompasses and generalizes various quantum optics and waveguide QED master equations with particular focus on giant atoms and decoherence-free Hamiltonians. As such, it could be skipped by a reader solely interested in the collision-model derivation.

For a single normal emitter,  $N_e = \mathcal{N} = 1$ ,  $\hat{A}_1 \equiv \hat{A}$  (setting  $x_1 = \tau_1 = 0$ ), and  $\hat{H}_{\text{vac}} = 0$ . Thus the ME (23) [or (28) for  $\gamma' = 0$ ] reduces to the well-known general ME of quantum optics for a pointlike atom or harmonic oscillator [54]. For a pair of normal emitters coupled to a unidirectional field, we have  $N_e = \mathcal{N} = 2$  and  $\hat{A}_\nu \equiv e^{-i\omega_0\tau_\nu} \hat{A}_\nu = e^{-ik_0x_\nu} \hat{A}_\nu$ , with  $\nu = 1, 2$  (operators with different  $\nu$ 's in this case commute). Hence,  $\hat{H}_{\text{vac}} = i\frac{\gamma}{2}(\hat{A}_1^\dagger \hat{A}_2 - \hat{A}_2^\dagger \hat{A}_1)$  and  $\hat{A} = \hat{A}_1 + \hat{A}_2$  so that for  $\alpha_i = N = M = 0$  (vacuum) Eq. (23) [or (28) for  $\gamma' = 0$ ] reduces to the well-known ME of a pair of cascaded emitters in vacuum [56,57].

For  $N_e = \mathcal{N}$  normal emitters coupled to a bidirectional field (such that  $\gamma' = \gamma = \Gamma/2$ ) Eq. (28) reduces to

$$\begin{aligned} \dot{\rho} = & -i\frac{\Gamma}{2} \sum_{i \neq j} \sin(k_0 x_{ij}^-) [\hat{A}_i^\dagger \hat{A}_j, \rho] \\ & + \Gamma(N+1) \sum_{ij} \cos(k_0 x_{ij}^-) (\hat{A}_i \rho \hat{A}_j^\dagger - \frac{1}{2} [\hat{A}_j^\dagger \hat{A}_i, \rho]_+) \\ & + \Gamma N \sum_{ij} \cos(k_0 x_{ij}^-) (\hat{A}_i^\dagger \rho \hat{A}_j - \frac{1}{2} [\hat{A}_j \hat{A}_i^\dagger, \rho]_+) \\ & + \Gamma \sum_{ij} \cos(k_0 x_{ij}^+) \{M(\hat{A}_i^\dagger \rho \hat{A}_j^\dagger - \frac{1}{2} [\hat{A}_j^\dagger \hat{A}_i^\dagger, \rho]_+) + \text{H.c.}\}, \end{aligned} \quad (40)$$

where  $x_{ij}^\pm = x_j \pm x_i$  and we used that  $\hat{A}_j = \hat{A}_j e^{-ik_0x_j}$  and  $\hat{A}'_j = \hat{A}_j e^{ik_0x_j}$  (atom and coupling-point indices coincide). For  $N = N' = \sinh^2(|\xi|)$  and  $M = M' = e^{-i\theta} \sinh(|\xi|) \cosh(|\xi|)$

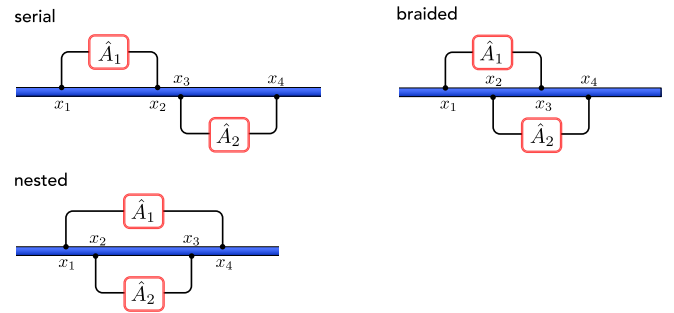


FIG. 5. Possible topologies for the pattern of coupling points of two giant emitters: serial, nested, and braided. We used the single index  $\nu = 1, \dots, 4$  to label the coupling points.

Eq. (40) reduces to the master equation found through standard methods in Ref. [58] ( $\xi = |\xi|e^{-i\theta}$  is the squeezing parameter, where  $\theta$  can include contributions depending on the distance from the source). For zero squeezing  $\xi = N = M = 0$ , Eq. (40) reduces to the standard waveguide QED master equation of a set of atoms [59,60]. Thus Eq. (28) generalizes the squeezed-bath master equation to giant emitters.

For a single giant emitter with two coupling points in a bidirectional waveguide,  $\gamma' = \gamma = \Gamma/2$  (with  $\Gamma$  the total decay rate),  $N_e = 1$ ,  $\mathcal{N} = 2$ ,  $\hat{A}_1 = \hat{A}'_1 = \hat{A}_1 = \hat{A}$ ,  $\hat{A}_2 = e^{-i\varphi} \hat{A}$ , and  $\hat{A}'_2 = e^{i\varphi} \hat{A}$ , where we set  $x_1 = \tau_1 = 0$  and  $\varphi = k_0 x_2 = \omega_0 \tau_2$  ( $\hat{A}$  could be a spin-1/2 or bosonic ladder operator). The collective operators (27) thus read

$$\hat{A} = (1 + e^{-i\varphi})\hat{A}, \quad \hat{A}' = (1 + e^{+i\varphi})\hat{A}. \quad (41)$$

Plugging these into Eq. (28), for  $\alpha_i = \alpha'_i = N = N' = M = M' = 0$  we retrieve the vacuum master equation [51,61]

$$\dot{\rho} = -i\frac{\Gamma}{2} \sin \varphi [\hat{A}^\dagger \hat{A}, \rho] + \Gamma(1 + \cos \varphi) \mathcal{D}_{\hat{A}}[\rho]. \quad (42)$$

For a pair of giant emitters with two coupling points each and a bidirectional waveguide,  $\gamma' = \gamma = \Gamma/2$ ,  $N_e = 2$ , and  $\mathcal{N} = 4$ . The  $\hat{A}_\nu$ 's and  $\hat{A}'_\nu$ 's depend on the pattern of coupling points, for which three different topologies are possible: serial, nested, and braided (see Fig. 5). Setting  $\varphi_\nu = k_0 x_\nu = \omega_0 \tau_\nu$  and as usual  $x_1 = \tau_1 = 0$ , in the braided configuration in particular one gets  $\hat{A}_1 = \hat{A}_1$ ,  $\hat{A}_2 = \hat{A}_2 e^{-i\varphi_2}$ ,  $\hat{A}_3 = \hat{A}_1 e^{-i\varphi_3}$ , and  $\hat{A}_4 = \hat{A}_2 e^{-i\varphi_4}$ . Hence [cf. Eq. (27)],

$$\hat{A} = (1 + e^{-i\varphi_3})\hat{A}_1 + (e^{-i\varphi_2} + e^{-i\varphi_4})\hat{A}_2, \quad (43)$$

while  $\hat{A}'$  has an analogous expression with  $\varphi_\nu \rightarrow -\varphi_\nu$ . Plugging these into (28), for  $\varphi_\nu = \nu\varphi$  (uniform spacings) and the field vacuum state, one gets

$$\begin{aligned} \dot{\rho} = & -i\frac{\Gamma}{2} (3 \sin \varphi + \sin 3\varphi) [\hat{A}_2^\dagger \hat{A}_1 + \hat{A}_1^\dagger \hat{A}_2, \rho] \\ & + 2\Gamma(1 + \cos 2\varphi) (\mathcal{D}_{\hat{A}_1}[\rho] + \mathcal{D}_{\hat{A}_2}[\rho]) \\ & + \Gamma(3 \cos \varphi + \cos 3\varphi) \sum_{i \neq j} (\hat{A}_i \rho \hat{A}_j^\dagger - \frac{1}{2} [\hat{A}_j^\dagger \hat{A}_i, \rho]_+), \end{aligned} \quad (44)$$

which was derived through the SLH formalism in Ref. [51] along with other master equations for different configurations

and numbers of atoms [these can all be retrieved from (28) likewise].

### Decoherence-free Hamiltonians with giant atoms

A major appeal of giant emitters is that they allow one to implement decoherence-free many-body Hamiltonians. A paradigmatic instance is the braided configuration in Fig. 5. By adjusting a  $\pi$ -phase shift between the coupling points of the same emitter, e.g., setting  $\varphi = \pi/2$ , all the dissipative terms in Eq. (44) vanish but the Hamiltonian  $\hat{H}_{\text{vac}}$ , which effectively seeds a dissipationless coherent interaction [51].

In the collisional picture this phenomenon can be predicted without working out the master equation, making clear at once that it occurs regardless of the field state [thus being not limited to the vacuum state assumed in the derivation of Eq. (44)]. Indeed, the condition that collective operators (27) vanish,

$$\hat{\mathcal{A}} = \hat{\mathcal{A}}' = 0 \quad (45)$$

(or just  $\hat{\mathcal{A}} = 0$  with a unidirectional field), guarantees that the joint emitter-field propagator reduces to  $\hat{U}_t = \exp(-i\hat{H}_{\text{vac}}t)$ . This is because (45) effectively decouples the emitters from the field time bins in light of Eqs. (14), (25), and (26), thus inhibiting dissipation. Having giant emitters is clearly indispensable since for normal emitters there is no way for  $\hat{\mathcal{A}}$  and  $\hat{\mathcal{A}}'$  to identically vanish in the entire Hilbert space. The question is now whether or not (45) yields in addition a null  $\hat{H}_{\text{vac}}$  (if so, no evolution takes place). For a giant atom [cf. Eq. (41)], the condition  $\hat{\mathcal{A}} = \hat{\mathcal{A}}' = 0$  holds for  $\varphi = (2n+1)\pi$ , which will also entail  $\hat{H}_{\text{vac}} = 0$ . For two giant atoms, the collective operators vanish for any  $\pi$ -phase shift between the coupling points of the same emitter [cf. Eq. (43)]. Using (25), one can check that this always yields  $\hat{H}_{\text{vac}} = 0$  in the serial and nested topologies (see Fig. 5), whereas in the braided one  $\hat{H}_{\text{vac}}$  can be nonzero (for a comprehensive analysis we point the reader to Ref. [62]).

In the collisional picture, the occurrence of  $\hat{H}_{\text{vac}} \neq 0$  with zero decoherence means that each time bin ends up uncorrelated with the emitters as the collision is complete. Notwithstanding, during the collision, it mediates a crosstalk between the emitters, which thus get correlated with one another.

## V. COLLISION MODEL DERIVATION

In this section we address the derivation of the collision model for a unidirectional field (the generalization to the bidirectional case is presented in Sec. VII).

Two regimes stand out: (i) negligible time delays, with  $\tau_{\mathcal{N}} - \tau_1 \ll \gamma^{-1}$  (hence  $\tau_{\mathcal{N}} - \tau_1$  can be replaced with  $\tau_\nu - \tau_{\nu-1}$  for all  $\nu$ 's), and (ii) non-negligible time delays, with a significant value of  $\gamma(\tau_\nu - \tau_{\nu-1})$  for any  $\nu$  (say, of the order of  $\sim 0.1$  or larger). Note that regime (i) is often dubbed Markovian. Strictly speaking, this is an abuse of language relying on the fact that for many typical field states (such as vacuum, thermal, coherent, or broadband squeezed states) dynamics in regime (i) are Markovian and described by a Lindblad master equation. This is not necessarily the case, though, with more general field states such as single-photon wave packets, even

for a single coupling point [63]. Intermediate regimes between (i) and (ii) are of course possible, but these can be described as a combination of (i) and (ii).

Most of the present section concerns the regime of negligible time delays (i) (our main focus in this work), which still occurs in the vast majority of experimental setups (see e.g., Ref. [64] for a discussion on circuit QED systems). Nevertheless, we begin with some general considerations and properties common to both regimes.

Consider a time mesh defined by  $t_n = n\Delta t$ , with  $n = 0, 1, \dots$  an integer and  $\Delta t$  the time step (later on this will be interpreted as the collision time). In the interaction picture (see Sec. II A), the propagator  $\hat{U}_t$  can be decomposed as<sup>2</sup>

$$\hat{U}_t = \hat{\mathcal{T}} \exp\left(-i \int_{t_0}^t ds \hat{V}_s\right) = \prod_{n=1}^{\lceil t/\Delta t \rceil} \hat{U}_n, \quad (46)$$

with  $\hat{V}_s$  given in Eq. (6) and  $\hat{\mathcal{T}}$  the usual time-ordering operator and where each unitary  $\hat{U}_n$  describes the evolution in the time interval  $t \in [t_{n-1}, t_n]$ ,

$$\hat{U}_n = \hat{\mathcal{T}} \exp\left(-i \int_{t_{n-1}}^{t_n} ds \hat{V}_s\right). \quad (47)$$

This discretization of the joint dynamics underpins the collision-model description (in any regime). Throughout, we will consider a time step much shorter than the characteristic interaction time, i.e.,  $\Delta t \ll \gamma^{-1}$ . Accordingly, we apply the Magnus expansion [65] and approximate (47) up to second order in  $\Delta t$  as

$$\hat{U}_n \simeq \mathbb{1} - i(\hat{\mathcal{H}}_n^{(0)} + \hat{\mathcal{H}}_n^{(1)})\Delta t - \frac{1}{2}(\hat{\mathcal{H}}_n^{(0)})^2\Delta t^2, \quad (48)$$

with  $\mathbb{1}$  the identity operator and

$$\hat{\mathcal{H}}_n^{(0)} = \frac{1}{\Delta t} \int_{t_{n-1}}^{t_n} ds \hat{V}_s, \quad (49)$$

$$\hat{\mathcal{H}}_n^{(1)} = \frac{i}{2\Delta t} \int_{t_{n-1}}^{t_n} ds \int_{t_{n-1}}^s ds' [\hat{V}_{s'}, \hat{V}_s] \quad (50)$$

(note that  $\hat{\mathcal{H}}_n^{(1)}$  is Hermitian). Using (8),  $\hat{\mathcal{H}}_n^{(0)}$  more explicitly reads

$$\begin{aligned} \hat{\mathcal{H}}_n^{(0)} &= \frac{1}{\Delta t} \int_{t_{n-1}}^{t_n} ds \sqrt{\gamma} \sum_{\nu} \hat{\mathcal{A}}_{\nu} \hat{b}_{s-\tau_{\nu}}^{\dagger} + \text{H.c.} \\ &= \sqrt{\frac{\gamma}{\Delta t}} \sum_{\nu} \hat{\mathcal{A}}_{\nu} \left( \frac{1}{\sqrt{\Delta t}} \int_{t_{n-1}-\tau_{\nu}}^{t_n-\tau_{\nu}} ds \hat{b}_s^{\dagger} \right) + \text{H.c.}, \end{aligned} \quad (51)$$

while  $\hat{\mathcal{H}}_n^{(1)}$  is the sum of three terms

$$\hat{\mathcal{H}}_n^{(1)} = \hat{\mathcal{H}}_{\text{vac}}^{(1)} + \hat{\mathcal{H}}_{\text{th}}^{(1)} + \hat{\mathcal{H}}_{\text{sq}}^{(1)}, \quad (52)$$

<sup>2</sup>In Eq. (46) we neglect the contribution coming from the interval between  $\lceil t/\Delta t \rceil \Delta t$  and  $t$  since this vanishes in the limit  $\Delta t \rightarrow 0$ .

with<sup>3</sup>

$$\hat{\mathcal{H}}_{\text{vac}}^{(1)} = i \frac{\gamma}{2\Delta t} \sum_{\nu\nu'} \hat{\mathcal{A}}_{\nu'}^\dagger \hat{\mathcal{A}}_\nu \int_{t_{n-1}}^{t_n} ds \int_{t_{n-1}}^s ds' [\hat{b}_{s'-\tau_{\nu'}}^\dagger, \hat{b}_{s-\tau_\nu}^\dagger] + \text{H.c.}, \quad (53)$$

$$\hat{\mathcal{H}}_{\text{th}}^{(1)} = i \frac{\gamma}{2\Delta t} \sum_{\nu\nu'} [\hat{\mathcal{A}}_{\nu'}^\dagger, \hat{\mathcal{A}}_\nu] \int_{t_{n-1}}^{t_n} ds \int_{t_{n-1}}^s ds' \hat{b}_{s'-\tau_{\nu'}}^\dagger \hat{b}_{s-\tau_\nu} + \text{H.c.}, \quad (54)$$

$$\hat{\mathcal{H}}_{\text{sq}}^{(1)} = i \frac{\gamma}{2\Delta t} \sum_{\nu\nu'} [\hat{\mathcal{A}}_{\nu'}, \hat{\mathcal{A}}_\nu] \int_{t_{n-1}}^{t_n} ds \int_{t_{n-1}}^s ds' \hat{b}_{s'-\tau_{\nu'}}^\dagger \hat{b}_{s-\tau_\nu}^\dagger + \text{H.c.} \quad (55)$$

### A. Negligible time delays

When time delays are negligible we can coarse grain the dynamics over a timescale defined by  $\Delta t$  such that

$$\tau_{\mathcal{N}} - \tau_1 \ll \Delta t \ll \gamma^{-1}, \quad (56)$$

meaning that the overall length of the coupling point array (hence the distance between any pair  $\tau_\nu - \tau_{\nu'}$ ) is negligible compared to the time step defining the timescale [see Fig. 3(a)]. We can take advantage of (56) and obtain approximated expressions of  $\hat{\mathcal{H}}_n^{(0)}$  and  $\hat{\mathcal{H}}_n^{(1)}$ . As for  $\hat{\mathcal{H}}_n^{(0)}$ , the lower and upper limits of integration of each integral appearing in (51) can be approximated as  $t_{n-1} - \tau_\nu \simeq t_{n-1}$  and  $t_n - \tau_\nu \simeq t_n$  so that (we set  $\tau_1 = 0$  throughout)

$$\int_{t_{n-1}-\tau_\nu}^{t_n-\tau_\nu} ds \hat{b}_s \simeq \int_{t_{n-1}}^{t_n} ds \hat{b}_s = \sqrt{\Delta t} \hat{b}_n, \quad (57)$$

where we defined the  $\hat{b}_n$ 's as in (17). It is easily checked that the commutation rules for the  $\hat{b}_t$ 's [cf. Eq. (5)] entail  $[\hat{b}_n, \hat{b}_m^\dagger] = \delta_{nm}$  and  $[\hat{b}_n, \hat{b}_m] = [\hat{b}_n^\dagger, \hat{b}_m^\dagger] = 0$ . Thus the  $\hat{b}_n$ 's define a discrete collection of bosonic modes, which we will usually refer to in the remainder as time-bin modes or at times simply as time bins. Thus (51) in the present regime reduces to

$$\hat{\mathcal{H}}_n^{(0)} \simeq \hat{V}_n = \sqrt{\frac{\gamma}{\Delta t}} (\hat{\mathcal{A}} \hat{b}_n^\dagger + \text{H.c.}), \quad (58)$$

where  $\hat{\mathcal{A}} = \sum_\nu \hat{\mathcal{A}}_\nu$  is a collective operator of the emitters. Note the characteristic scaling  $\sim \Delta t^{-1/2}$  of the emitter (time-bin) coupling strength, which is a hallmark of CMs [4].

In line with the approximation (57), in Eqs. (54) and (55) all time delays can be neglected, replacing  $s - \tau_\nu$  ( $s' - \tau_{\nu'}$ ) with  $s$  ( $s'$ ). Based on this, in Appendix B we show that both  $\hat{\mathcal{H}}_{\text{th}}^{(1)}$  and  $\hat{\mathcal{H}}_{\text{sq}}^{(1)}$  can be neglected (note that Appendix B refers to Sec. VB to be discussed shortly).

Thus we are left only with the vacuum contribution  $\hat{\mathcal{H}}_{\text{vac}}^{(1)}$ . To work this out, we first note that each double integral in

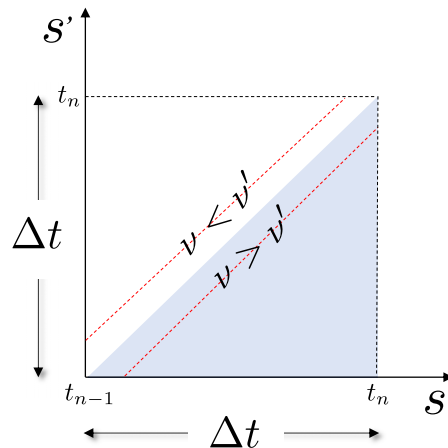


FIG. 6. Calculation of double integrals appearing in the vacuum term (53). The shaded region (triangle) represents the domain of integration. The integrand  $\delta(s' - s + (\tau_\nu - \tau_{\nu'}))$  vanishes everywhere except on the red line  $s' = s - (\tau_\nu - \tau_{\nu'})$ . This line lies within the triangular domain for  $\nu > \nu'$  and outside it for  $\nu < \nu'$ . Thereby, the integral is equal to  $\Delta t$  in the former case and vanishes in the latter.

Eq. (53) runs over the shaded triangle sketched in Fig. 6. For a given pair ( $\nu$  and  $\nu'$ ), the two-variable  $\delta$  function

$$[\hat{b}_{s'-\tau_{\nu'}}^\dagger, \hat{b}_{s-\tau_\nu}^\dagger] = \delta(s' - \tau_{\nu'} - s + \tau_\nu) \quad (59)$$

peaks on the line  $s' = s - (\tau_\nu - \tau_{\nu'})$ . As shown in Fig. 6, this line falls within the triangle for  $\nu > \nu'$  and outside it for  $\nu < \nu'$  (since  $\tau_\nu - \tau_{\nu'} > 0$  for  $\nu > \nu'$ ). Hence, only terms  $\nu > \nu'$  contribute to  $\hat{\mathcal{H}}_{\text{vac}}^{(1)}$  and we conclude that  $\hat{\mathcal{H}}_{\text{vac}}^{(1)} \equiv \hat{H}_{\text{vac}}$  [cf. Eq. (15)].

The above shows that for delays negligible with respect to  $\Delta t$ , which in turn is much shorter than the interaction characteristic timescale  $\gamma^{-1}$ , in Eq. (48) we can approximate  $\hat{\mathcal{H}}_n^{(0)} \simeq \hat{V}_n$  and  $\hat{\mathcal{H}}_n^{(1)} \simeq \hat{H}_{\text{vac}}$ . Thereby,

$$\hat{U}_n \simeq \mathbb{1} - i(\hat{H}_{\text{vac}} + \hat{V}_n)\Delta t - \frac{1}{2}\hat{V}_n^2\Delta t^2, \quad (60)$$

showing that in this regime the joint emitter-field dynamics can be effectively pictured as a sequence of short pairwise interactions (collisions) of duration  $\Delta t$  (collision time), as sketched in Figs. 1 and 3(a). In each interaction the emitters collectively couple to a fresh time bin (only one) according to the coupling Hamiltonian  $\hat{V}_n$  and at the same time coherently interact with one another through the second-order many-body Hamiltonian  $\hat{H}_{\text{vac}}$ . Note that time bins are uncoupled from one another and that each collides with the emitter only once in a conveyor-belt fashion (see Fig. 1).

As said, to arrive at Eq. (60), all time delays  $\tau_\nu - \tau_{\nu'}$  were neglected. We point out that this is different from setting  $\tau_\nu - \tau_{\nu'} = 0$ . Instead, it corresponds to performing the limit  $\tau_\nu - \tau_{\nu'} \rightarrow 0^+$  for all pairs ( $\nu, \nu'$ ) with  $\nu > \nu'$ . Indeed, it is easily checked that setting  $\tau_\nu - \tau_{\nu'} = 0$  entails  $\hat{\mathcal{H}}_{\text{vac}}^{(1)} = 0$  since in this case both terms  $\nu > \nu'$  and  $\nu < \nu'$  must be accounted for but exactly cancel out (the two dashed lines in Fig. 6 now both reduce to  $s' = s$ ). Physically, this means that the effective Hamiltonian  $\hat{H}_{\text{vac}}$  stems from the fact that, while traveling from left to right [see Fig. 3(a)], the  $n$ th time bin interacts *first* with coupling point  $\nu$  and only *afterward* with  $\nu + 1$ , no matter how short the delay  $\tau_{\nu+1} - \tau_\nu$ . This is in

<sup>3</sup>Subscripts vac, th, and sq come from vacuum, thermal, and squeezed. The corresponding Hamiltonian terms are indeed proportional to  $[b_t, b_t^\dagger]$ ,  $b_t^\dagger b_t$ , and  $b_t^\dagger b_t^\dagger$ , respectively, reflecting the fact that  $\hat{\mathcal{H}}_{\text{vac}}^{(1)}$  arises for any field state, while typical field states for which  $\hat{\mathcal{H}}_{\text{th}}^{(1)}$  ( $\hat{\mathcal{H}}_{\text{sq}}^{(1)}$ ) occurs are thermal (squeezed) states.

line with similar observations made in derivations of cascaded MEs through other methods (see, e.g., [56]). Interestingly, the collisional picture allows for a complementary interpretation of this phenomenon in terms of far-detuned time-bin modes  $\hat{b}_{n,k}$ , which we introduce next.

### B. Time-bin modes $\hat{b}_{n,k}$

It should be clear from the definition (17) that, for a finite  $\Delta t$ , modes  $\hat{b}_n$  generally capture only part of the field degrees of freedom. Formally, this can be seen by expanding the continuous-time modes as [8]

$$\hat{b}_t = \frac{1}{\sqrt{\Delta t}} \sum_n \sum_{k=-\infty}^{\infty} \Theta_n(t) e^{-i2\pi kt/\Delta t} \hat{b}_{n,k}, \quad (61)$$

with  $\Theta_n(t) = 1$  for  $t \in [t_{n-1}, t_n]$  and 0 otherwise and where

$$\hat{b}_{n,k} = \frac{1}{\sqrt{\Delta t}} \int_{t_{n-1}}^{t_n} dt e^{i2\pi kt/\Delta t} b_t. \quad (62)$$

Ladder operators  $\hat{b}_{n,k}$  fulfill  $[\hat{b}_{n,k}, \hat{b}_{n',k'}^\dagger] = \delta_{n,n'} \delta_{k,k'}$  and  $[\hat{b}_{n,k}, \hat{b}_{n',k'}] = [\hat{b}_{n,k}^\dagger, \hat{b}_{n',k'}^\dagger] = 0$ . Moreover, for  $k=0$  we retrieve modes  $\hat{b}_n$  [cf. Eq. (17)], i.e.,  $\hat{b}_{n,0} \equiv \hat{b}_n$ . A straightforward Fourier analysis shows that time-bin modes  $\hat{b}_{n,k \neq 0}$  are dominated by field normal modes whose detunings from the emitter grow as  $\sim |k|/\Delta t$  (while modes  $\hat{b}_{n,0}$  contain field frequencies quasis resonant with the emitter) [8]. For  $\Delta t \rightarrow 0$  [still fulfilling (56)], corresponding to the continuous-time limit of the dynamics, these frequencies become divergent. Accordingly, it is reasonable to assume there are no photons populating modes  $\hat{b}_{n,k \neq 0}$ . This is equivalent to stating that the most general field state is of the form

$$\rho_f = \eta_{\text{bins}} \bigotimes_{n,k \neq 0} |0\rangle_{n,k} \langle 0|, \quad (63)$$

with  $\eta_{\text{bins}}$  the (generally mixed) state of modes  $\hat{b}_n \equiv \hat{b}_{n,0}$  and  $|0\rangle_{n,k}$  the vacuum state of mode  $\hat{b}_{n,k}$ .

### C. Differences with the single-coupling-point case

For a single coupling point ( $\mathcal{N} = 1$ )  $\hat{H}_{\text{vac}}$  of course does not arise and we are only left with  $\hat{V}_n$  (containing only  $\hat{b}_n \equiv \hat{b}_{n,0}$ ), meaning that the coupling to time-bin modes  $k \neq 0$  is negligible. However, for two or more coupling points ( $\mathcal{N} \geq 2$ ), these off-resonant modes yield non-negligible effects despite them not explicitly appearing in  $\hat{H}_{\text{vac}}$  (not even in  $\hat{V}_n$ , of course). Indeed, they are in fact responsible for the emergence of  $\hat{H}_{\text{vac}}$ . This can be seen from Eq. (53) featuring a singularity in the integrand function due to the field commutator. Such a singular behavior forbids retention of only  $k=0$  terms in expansion (61) no matter how small  $\Delta t$  is [indeed, it is easily checked that expanding each field operator entering Eq. (53) and retaining only modes  $\hat{b}_{n,0} = \hat{b}_n$  would yield a vanishing  $\hat{H}_{\text{vac}}$ ].

Thus all time-bin modes  $\hat{b}_{n,k}$  in fact contribute to the dynamics for  $\mathcal{N} > 1$ . However, unlike  $k=0$  modes, off-resonant modes  $k \neq 0$  are only virtually excited, explaining why they do not explicitly appear in  $\hat{H}_{\text{vac}}$ .

### D. Non-negligible time delays

A comprehensive treatment of the regime of non-negligible delays is beyond the scope of the present paper. However, we wish to highlight a major difference from the negligible delay regime, that at each time step the emitters collide with as many time bins as the number of coupling points (instead of only one). To illustrate this, we work out next  $\hat{\mathcal{H}}_n^{(0)}$  [cf. Eq. (49) and its equivalent expression (51)].

In contrast with the negligible delay regime, now one can take a time step negligible compared with all the system's time delay, i.e.,  $\Delta t \ll \tau_\nu - \tau_{\nu-1}$  for all  $\nu$  (note that this is compatible with the condition  $\Delta t \ll \gamma^{-1}$  that we assume throughout). For sufficiently short  $\Delta t$ , the coupling point coordinates can be discretized as  $\tau_\nu = m_\nu \Delta t$ , where  $\{m_\nu\}$  are  $\mathcal{N}$  integers such that  $m_1 < m_2 < \dots < m_{\mathcal{N}}$ , and set  $\tau_1 = m_1 = 0$ . Accordingly, (51) becomes (recall that  $t_n = n \Delta t$ )

$$\hat{\mathcal{H}}_n^{(0)} = \sqrt{\frac{\gamma}{\Delta t}} \sum_\nu (\hat{\mathcal{A}}_\nu \hat{b}_{n-m_\nu}^\dagger + \text{H.c.}), \quad (64)$$

showing that, during a given time interval  $[t_{n-1}, t_n]$ , each coupling point  $\nu$  interacts with a different time bin  $n - m_\nu$  [see Fig. 3(b)].

In the presence of giant emitters (even a single one), this dynamics is tough to tackle analytically. Through an elegant diagrammatic technique, Grimsmo found an analytical solution for the open dynamics of a driven giant atom with two coupling points [2], while Pichler and Zoller found an efficient matrix-product-state approach which they applied to a pair of driven normal atoms coupled to a bidirectional field [1] (the collisional picture for a bidirectional field is addressed in Sec. VII). A major reason behind the complexity of this dynamics lies in its generally non-Markovian nature (conditions for Markovian behavior are discussed in Sec. VI).

## VI. MASTER EQUATION FOR NEGLIGIBLE TIME DELAYS

In Sec. VA we focused on the total propagator, showing that for negligible time delays it can be decomposed as a sequence of collisions between the emitters (jointly) and a field time bin, each described by the two-body elementary unitary  $\hat{U}_n$  in Eq. (60), which is fully specified by  $\hat{H}_{\text{vac}}$  and  $\hat{V}_n$ . In this section we derive master equations for the emitters and time bin in the regime of negligible time delays.

### A. Conditions for Markovian dynamics

Based on (63) and the related discussion, from now on time-bin modes  $\hat{b}_{n,k \neq 0}$  will be ignored. The joint state of the emitters and *all* time bins (modes  $\hat{b}_n \equiv \hat{b}_{n,0}$ ) evolves at each time step as  $\sigma_n = \hat{U}_n \sigma_{n-1} \hat{U}_n^\dagger$ , with  $\sigma_n = \sigma_{t=t_n}$ . A corresponding finite-difference equation of motion is worked out by replacing  $\hat{U}_n$  with (60) and retaining only terms up to second order in  $\Delta t$ ,

$$\begin{aligned} \frac{\Delta \sigma_n}{\Delta t} = & -i[\hat{H}_{\text{vac}} + \hat{V}_n, \sigma_{n-1}] \\ & + \Delta t (\hat{V}_n \sigma_{n-1} \hat{V}_n - \frac{1}{2} [\hat{V}_n^2, \sigma_{n-1}]_+), \end{aligned} \quad (65)$$

where  $\Delta\sigma_n = \sigma_n - \sigma_{n-1}$  (recall that  $\hat{V}_n \sim 1/\sqrt{\Delta t}$ ). Under the usual assumption of zero initial correlations between the emitters and the field, the initial condition reads  $\sigma_0 = \rho_0 \otimes \eta_{\text{bins}}$ , where  $\rho_0$  and  $\eta_{\text{bins}}$  are the initial states of all emitters and all time bins, respectively.

We next ask whether or not the reduced dynamics of the emitters  $\rho_n = \text{Tr}_{\text{bins}}\{\sigma_n\}$  is Markovian and describable by a Lindblad master equation. We note that this is generally not the case when time bins are initially correlated, namely,  $\eta_{\text{bins}}$  is not a product state, since in these conditions the emitters can get correlated with a time bin even before colliding with it [4,27]. This indeed rules out that the evolution of the emitters (open system) at each elementary collision be described by a CPTP quantum map [66], which is the key requirement for a Lindblad master equation to hold. A typical instance is a single-photon wave packet of bandwidth comparable to  $\gamma$  [10,12,13,63,67].

We thus consider the case that time bins are initially uncorrelated, that is,

$$\eta_{\text{bins}} = \bigotimes_n \eta_n, \quad (66)$$

with  $\eta_n$  the reduced state of the  $n$ th time bin mode having ladder operator  $\hat{b}_n = \hat{b}_{n,0}$ . This entails

$$\rho_n = \text{Tr}_{\text{bins}}\{\hat{U}_n \sigma_{n-1} \hat{U}_n^\dagger\} = \text{Tr}_n\{\hat{U}_n \rho_{n-1} \eta_n \hat{U}_n^\dagger\}, \quad (67)$$

where  $\text{Tr}_n$  is the partial trace over the time bin  $n$  (mode  $\hat{b}_n \equiv \hat{b}_{n,0}$ ). This defines a CPTP map describing how the emitters' state  $\rho_n$  is changed by the  $n$ th collision. Likewise, the  $n$ th time bin evolves according to

$$\eta'_n = \text{Tr}_S\{\hat{U}_n \rho_{n-1} \eta_n \hat{U}_n^\dagger\}, \quad (68)$$

with  $\text{Tr}_S$  the partial trace over the emitters. This is a CPTP map describing the change of the single time-bin state due to collision with the emitters (after the collision this state will no longer change since time bins are noninteracting). Note that the map (68) depends parametrically on the current reduced state of emitters (updated at each collision).

### B. Master equation for the emitters

To work out the Lindblad master equation of the emitters corresponding to the map (67) we simply trace off all time bins from Eq. (65), which yields

$$\frac{\Delta\rho_n}{\Delta t} = -i[\hat{H}_{\text{vac}} + \langle\hat{V}_n\rangle, \rho_{n-1}] + \mathcal{D}[\rho_{n-1}], \quad (69)$$

with  $\langle\cdots\rangle = \text{Tr}_n\{\cdots \eta_n\}$ ,  $\Delta\rho_n = \rho_n - \rho_{n-1}$ , and

$$\mathcal{D}[\rho_{n-1}] = \Delta t \text{Tr}_n\{\hat{V}_n \rho_{n-1} \eta_n \hat{V}_n - \frac{1}{2}[\hat{V}_n^2, \rho_{n-1} \eta_n]_+\}. \quad (70)$$

Although not explicit, this equation is in Lindblad form, as is easily checked by spectrally decomposing  $\eta_n$  (see, e.g., Sec. 2.1.1 in Ref. [4]). The Lindblad form is guaranteed by the fact that the emitter evolution at each collision is described by a CPTP map [last identity in Eq. (67)].

Using (16), the first-order Hamiltonian and second-order dissipator can be put in the more explicit form

$$\langle\hat{V}_n\rangle = \sqrt{\frac{\gamma}{\Delta t}} (\langle\hat{b}_n\rangle \hat{A}^\dagger + \text{H.c.}), \quad (71)$$

$$\mathcal{D}[\rho_{n-1}] = \gamma \sum_{\mu\mu'} \langle\hat{c}_\mu \hat{c}_{\mu'}\rangle (\hat{c}_{\mu'} \rho_{n-1} \hat{c}_\mu - \frac{1}{2}[\hat{c}_\mu \hat{c}_{\mu'}, \rho_{n-1}]_+), \quad (72)$$

with  $\mu, \mu' = 1, 2$  and where we set

$$\hat{c}_1 = \hat{b}_n, \quad \hat{c}_2 = \hat{b}_n^\dagger, \quad \hat{C}_1 = \hat{A}^\dagger, \quad \hat{C}_2 = \hat{A}. \quad (73)$$

Now Eq. (69) is expressed fully in terms of the time-bin moments  $\langle\hat{b}_n\rangle$ ,  $\langle\hat{b}_n^\dagger \hat{b}_n\rangle$ , and  $\langle\hat{b}_n^2\rangle$ , which depend on  $\eta_n$ , which in turn is dependent on the initial field state [cf. Eq. (66)].

The time-bin moments can be determined for the most general white-noise Gaussian state of the field. As anticipated in Sec. III, such a state is fully specified by the first and second moments (21) [54]. Noting that  $\hat{b}_n = \int_{t_{n-1}}^{t_n} db_t / \sqrt{\Delta t}$ , it is evident that for such a field state,  $\langle\hat{b}_n^\dagger \hat{b}_{n'}\rangle = \langle\hat{b}_n \hat{b}_{n'}\rangle = 0$  for  $n \neq n'$ . This, because of the Gaussianity hypothesis, is equivalent to Eq. (66). Thus time bins are initially uncorrelated. Their first and second moments are given by (22), where the rigorous  $\alpha_n$ 's definition is  $\alpha_n = \int_{t_{n-1}}^{t_n} dt \alpha_t / \Delta t$  (for  $\Delta t$  short enough, this reduces to  $\alpha_n \simeq \alpha_{t_n}$ ). Note that  $\langle\hat{b}_n\rangle \propto \sqrt{\Delta t}$ , which cancels the  $1/\sqrt{\Delta t}$  factor in Eq. (71). Plugging moments (22) into the finite-difference equation (69) and taking the continuous-time limit such that  $\gamma \Delta t \rightarrow 0$ ,  $t_n \rightarrow t$ ,  $\rho_{n-1} \rightarrow \rho_t$ , and  $\Delta\rho_n / \Delta t \rightarrow d\rho/dt$ , we end up with the general master equation (23).

### C. Time-bin master equation

An equation for the rate of change of the single time-bin state,  $\Delta\eta_n / \Delta t$  with  $\Delta\eta_n = \eta'_n - \eta_n$ , can be similarly worked out. We again start from Eq. (65) but now trace over all emitters and all time bins  $n' \neq n$ , obtaining

$$\frac{\Delta\eta_n}{\Delta t} = -i[\langle\hat{V}_n\rangle_\rho, \eta_n] + \mathcal{D}_\rho[\eta_n], \quad (74)$$

with  $\langle\cdots\rangle_\rho = \text{Tr}_S\{\cdots \rho\}$  and

$$\mathcal{D}_\rho[\eta_n] = \Delta t \text{Tr}_S\{\hat{V}_n \rho_{n-1} \eta_n \hat{V}_n - \frac{1}{2}[\hat{V}_n^2, \rho_{n-1} \eta_n]_+\}, \quad (75)$$

where  $\text{Tr}_S\{\cdots\}$  is the partial trace over the system. Note that this equation parametrically depends on the state of the emitters,  $\rho_{n-1}$ , which changes at each time step. Equation (74) expresses the map (68) in the short-collision-time limit.

## VII. COLLISION MODEL FOR A BIDIRECTIONAL FIELD

For a bidirectional field (see Sec. II B), unitaries  $\hat{U}_t$  and  $\hat{U}_n$  are formally the same as (46) and (47), respectively, but  $\hat{V}_t$  is now given by Eq. (12). The  $\hat{U}_n$ 's lowest-order expansion (48) is formally unchanged. Through a reasoning analogous to that in Sec. V, in light of (12), Eqs. (51) and (52) are generalized as

$$\begin{aligned} \hat{\mathcal{H}}_n^{(0)} &= \sqrt{\frac{\gamma}{\Delta t}} \sum_v \hat{A}_v \left( \frac{1}{\sqrt{\Delta t}} \int_{t_{n-1}}^{t_n} ds \hat{b}_{s-\tau_v}^\dagger \right) \\ &\quad + \sqrt{\frac{\gamma'}{\Delta t}} \sum_v \hat{A}'_v \left( \frac{1}{\sqrt{\Delta t}} \int_{t_{n-1}}^{t_n} ds \hat{b}_{s+\tau_v}^\dagger \right) + \text{H.c.}, \quad (76) \\ \hat{\mathcal{H}}_n^{(1)} &= \hat{\mathcal{H}}_{\text{sq}}^{(1)} + \hat{\mathcal{H}}_{\text{th}}^{(1)} + \hat{\mathcal{H}}_{\text{vac}}^{(1)}, \quad (77) \end{aligned}$$

with

$$\hat{\mathcal{H}}_{\text{vac}}^{(1)} = \frac{i}{2\Delta t} \sum_{\nu, \nu'} \hat{\mathcal{A}}_{\nu'}^\dagger \hat{\mathcal{A}}_{\nu} \int_{t_{n-1}}^{t_n} ds \int_{t_{n-1}}^s ds' (\gamma [\hat{b}_{s'-\tau_{\nu'}}^\dagger, \hat{b}_{s-\tau_{\nu}}^\dagger] + \gamma' [\hat{b}_{s'+\tau_{\nu'}}^\dagger, \hat{b}_{s+\tau_{\nu}}^\dagger] - \text{H.c.}), \quad (78)$$

$$\begin{aligned} \hat{\mathcal{H}}_{\text{th}}^{(1)} &= \frac{i}{2\Delta t} \sum_{\nu, \nu'} \int_{t_{n-1}}^{t_n} ds \int_{t_{n-1}}^s ds' (\gamma [\hat{\mathcal{A}}_{\nu'}^\dagger, \hat{\mathcal{A}}_{\nu}] \hat{b}_{s-\tau_{\nu}}^\dagger \hat{b}_{s'-\tau_{\nu'}}^\dagger + \gamma' [\hat{\mathcal{A}}_{\nu'}^\dagger, \hat{\mathcal{A}}_{\nu}] \hat{b}_{s+\tau_{\nu}}^\dagger \hat{b}_{s'+\tau_{\nu'}}^\dagger - \text{H.c.}) \\ &+ \frac{i}{2\Delta t} \sqrt{\gamma\gamma'} \sum_{\nu, \nu'} \int_{t_{n-1}}^{t_n} ds \int_{t_{n-1}}^s ds' ([\mathcal{A}_{\nu'}^\dagger, \mathcal{A}_{\nu'}] \hat{b}_{s-\tau_{\nu}} \hat{b}_{s'+\tau_{\nu'}}^\dagger + [\mathcal{A}_{\nu'}^\dagger, \mathcal{A}_{\nu'}] \hat{b}_{s'-\tau_{\nu'}} \hat{b}_{s+\tau_{\nu}} - \text{H.c.}), \end{aligned} \quad (79)$$

$$\begin{aligned} \hat{\mathcal{H}}_{\text{sq}}^{(1)} &= \frac{i}{2\Delta t} \sum_{\nu, \nu'} \int_{t_{n-1}}^{t_n} ds \int_{t_{n-1}}^s ds' (\gamma [\hat{\mathcal{A}}_{\nu'}^\dagger, \hat{\mathcal{A}}_{\nu}] \hat{b}_{s-\tau_{\nu}}^\dagger \hat{b}_{s'-\tau_{\nu'}}^\dagger + \gamma' [\hat{\mathcal{A}}_{\nu'}^\dagger, \hat{\mathcal{A}}_{\nu}] \hat{b}_{s+\tau_{\nu}}^\dagger \hat{b}_{s'+\tau_{\nu'}}^\dagger - \text{H.c.}) \\ &+ \frac{i}{2\Delta t} \sqrt{\gamma\gamma'} \sum_{\nu, \nu'} \int_{t_{n-1}}^{t_n} ds \int_{t_{n-1}}^s ds' ([\mathcal{A}_{\nu'}^\dagger, \mathcal{A}_{\nu'}] \hat{b}_{s-\tau_{\nu}} \hat{b}_{s'+\tau_{\nu'}}^\dagger + [\mathcal{A}_{\nu'}^\dagger, \mathcal{A}_{\nu'}] \hat{b}_{s'-\tau_{\nu'}} \hat{b}_{s+\tau_{\nu}} - \text{H.c.}). \end{aligned} \quad (80)$$

### A. Negligible time delays

Regarding  $\hat{\mathcal{H}}_n^{(0)}$ , an argument analogous to that leading to (58) now yields that in the present regime  $\hat{\mathcal{H}}_n^{(0)} \simeq \hat{V}_n$ , with  $\hat{V}_n$  given by Eq. (26). Regarding  $\hat{\mathcal{H}}_n^{(1)}$ , as in the unidirectional case, the terms  $\hat{\mathcal{H}}_{\text{th}}^{(1)}$  and  $\hat{\mathcal{H}}_{\text{sq}}^{(1)}$  are again negligible in the limit of vanishing delays (see Appendix B). Compared to the unidirectional case [cf. Eq. (53)],  $\hat{\mathcal{H}}_{\text{vac}}^{(1)}$  has an extra term, due to the left-going modes, featuring the  $\delta$  function  $[\hat{b}_{s'+\tau_{\nu'}}^\dagger, \hat{b}_{s+\tau_{\nu}}^\dagger]$ . This peaks on the line  $s' = s - (\tau_{\nu'} - \tau_{\nu})$ , which differs from the  $\delta$  function coming from right-going modes [cf. Eq. (59)] for the exchange  $\nu \leftrightarrow \nu'$ . Accordingly, in Fig. 6, the lines corresponding to  $\nu < \nu'$  and  $\nu > \nu'$  are swapped; hence now only terms  $\nu < \nu'$  (instead of  $\nu > \nu'$ ) contribute to  $\hat{\mathcal{H}}_{\text{vac}}^{(1)}$ . Thus we end up with  $\hat{\mathcal{H}}_{\text{vac}}^{(1)} \equiv \hat{H}_{\text{vac}}$ , with  $\hat{H}_{\text{vac}}$  given by Eq. (25).

Thereby, for  $\tau_{\mathcal{N}} - \tau_1 \ll \Delta t \ll (1/\gamma, 1/\gamma')$ , the joint dynamics can be represented by an effective collision model (see Fig. 4), where at each collision the emitters jointly collide with a right-going and a left-going time bin, at once being subject to an internal coherent dynamics governed by the second-order Hamiltonian (25). Note that, formally, this can still be thought of as a collision model featuring a single stream of time bins (like in Fig. 1) provided one defines a two-mode time bin ( $\hat{b}_n$  and  $\hat{b}'_n$ ).

### B. Non-negligible time delays

An argument analogous to that used in Sec. VD generalizes Eq. (64) as

$$\hat{\mathcal{H}}_n^{(0)} = \frac{1}{\sqrt{\Delta t}} \sum_{\nu} (\sqrt{\gamma} \hat{\mathcal{A}}_{\nu} \hat{b}_{n-m_{\nu}}^\dagger + \sqrt{\gamma'} \hat{\mathcal{A}}_{\nu} \hat{b}'_{n+m_{\nu}} + \text{H.c.}). \quad (81)$$

Here ladder operators  $\hat{b}'_n$  [cf. Eq. (24)] define a discrete collection of left-going bosonic modes analogous to  $\hat{b}_n$  (the former commuting with the latter). Note the different subscripts in  $\hat{b}_{n-m_{\nu}}$  and  $\hat{b}'_{n+m_{\nu}}$ , reflecting that right- and left-going time bins travel in opposite directions, as sketched in Fig. 7. Similarly to the unidirectional case discussed in Sec. VD, analytical descriptions of this dynamics are demanding [1,68,69].

## VIII. MASTER EQUATION FOR A BIDIRECTIONAL FIELD

With the extended definitions of  $\hat{H}_{\text{vac}}$  and  $\hat{V}_n$  for a bidirectional field discussed in the preceding section (regime of negligible time delays), the finite-difference equation of motion (65) for the joint dynamics still holds. The initial state of the time bins  $\eta_{\text{bins}}$  is obtained from the initial field state by using (61) and tracing off time-bin modes  $k \neq 0$  (with left-going time-bin modes  $\hat{b}'_{n,k}$  also accounted for).

Likewise, a Markovian open dynamics will arise in the case of field states, which in the collisional picture turn into uncorrelated states of the time bins

$$\eta_{\text{bins}} = \bigotimes_n (\eta_{r,n} \otimes \eta_{l,n}), \quad (82)$$

with  $\eta_{r,n}$  ( $\eta_{l,n}$ ) the reduced state of the  $n$ th right-going (left-going) time bin. Preparing such states, the emitters evolve at each collision according to a CPTP map [cf. Eq. (67)] and so do time bins [see Eq. (68)].

The finite-difference master equation of the emitters (69) holds, where  $\langle \hat{V}_n \rangle$  and  $\mathcal{D}[\rho_{n-1}]$  are now given by

$$\langle \hat{V}_n \rangle = \sqrt{\frac{1}{\Delta t}} (\sqrt{\gamma} \langle \hat{b}_n \rangle \hat{\mathcal{A}}^\dagger + \sqrt{\gamma'} \langle \hat{b}'_n \rangle \hat{\mathcal{A}}'^\dagger + \text{H.c.}), \quad (83)$$

$$\mathcal{D}[\rho_{n-1}] = \mathcal{D}_r[\rho_{n-1}] + \mathcal{D}_l[\rho_{n-1}], \quad (84)$$

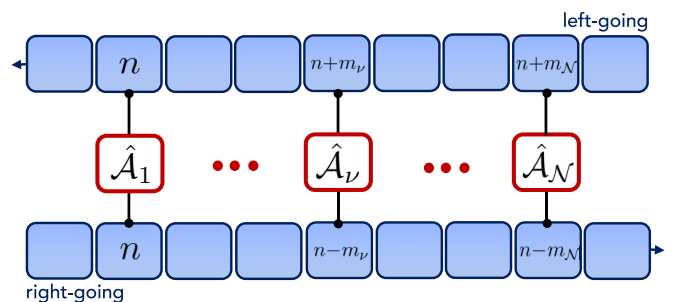


FIG. 7. Bidirectional field for non-negligible time delays: left-going time bins (top) and right-going time bins (bottom). We set  $\tau_1 = m_1 = 0$ .

with  $\mathcal{D}_r[\dots]$  the same as (72) and  $\mathcal{D}_l[\dots]$  obtained from (72) through the replacements  $\gamma \rightarrow \gamma'$ ,  $\hat{b}_n \rightarrow \hat{b}'_n$ , and  $\hat{A} \rightarrow \hat{A}'$ . The master equation is expressed in terms of the first and second moments of right-going and left-going time bins depending on  $\eta_{r,n}$  and  $\eta_{l,n}$ , respectively [cf. Eq. (82)].

The most general white-noise Gaussian state of the field is now specified by right-going moments (21) plus the analogously defined left-going moments  $\alpha'_l$ ,  $N'$ , and  $M'$ . The latter determine the time-bin moments  $\langle \hat{b}'_n \rangle = \alpha'_n \sqrt{\Delta t}$ ,  $\langle \hat{b}'_n \hat{b}'_n \rangle = N'$ , and  $\langle \hat{b}'_n{}^2 \rangle = M'$ . Plugging these into the finite-difference equation (69) and taking next the continuous-time limit as done in the unidirectional case, we end up with the master equation (28).

$$\tilde{\sigma}_n = |k_n\rangle\langle k_n| \hat{U}_n \cdots |k_1\rangle\langle k_1| \hat{U}_1 \left( \rho_0 \bigotimes_m \eta_m \right) \hat{U}_1^\dagger |k_1\rangle\langle k_1| \cdots \hat{U}_n^\dagger |k_n\rangle\langle k_n|, \quad (85)$$

with  $\hat{U}_n$  given by Eq. (60). The probability  $p_{k_1 \dots k_n}$  of getting this sequence of measurement outcomes is the norm of  $\tilde{\sigma}_n$ ,

$$p_{k_1 \dots k_n} = \text{Tr}\{\tilde{\sigma}_n\}; \quad (86)$$

hence the normalized state is  $\sigma_n = \tilde{\sigma}_n / p_{k_1 \dots k_n}$ .

Let each time bin be initially in a pure state  $\eta_m = |\chi_m\rangle\langle \chi_m|$  (the mixed case is discussed later). Plugging this into (85) and tracing off all the time bins yields (29), i.e., the unnormalized state of the emitters  $S$  at step  $n$  (while time bins are of course in state  $|k_1\rangle \cdots |k_n\rangle$ , uncorrelated with  $S$ ). Kraus operators  $\hat{K}_{k_m}$  [cf. (30)] are reported here again for convenience

$$\hat{K}_{k_m} = \langle k_m | \hat{U}_m | \chi_m \rangle. \quad (87)$$

Thus, since  $\text{Tr}_n\{\tilde{\sigma}_n\} = \text{Tr}_S\{\tilde{\rho}_n\}$ ,  $p_{k_1 \dots k_n}$  can be expressed as [cf. Eq. (86)]

$$p_{k_1 \dots k_n} = \text{Tr}_S\{\hat{K}_{k_n} \cdots \hat{K}_{k_1} \rho_0 \hat{K}_{k_1}^\dagger \cdots \hat{K}_{k_n}^\dagger\}. \quad (88)$$

As anticipated in Sec. III C, time-bin measurement with outcome  $k$  (at the end of the  $n$ th collision) thus projects the emitters into the (unnormalized) state

$$\tilde{\rho}_n = \hat{K}_k \rho_{n-1} \hat{K}_k^\dagger \quad (89)$$

with probability

$$p_k = \text{Tr}_S\{\tilde{\rho}_n\} = \text{Tr}_S\{\hat{K}_k^\dagger \hat{K}_k \rho_{n-1}\}. \quad (90)$$

As usual,  $\rho_{n-1}$  denotes the normalized state of  $S$  right before collision with time bin  $n$ . This map defines the conditional dynamics. Summing next over all possible  $k$ 's yields  $\rho_n = \sum_k \hat{K}_k \rho_{n-1} \hat{K}_k^\dagger$ , this CPTP map defining the unconditional open dynamics.

We derive next the lowest-order expansion of each Kraus operator  $\hat{K}_k$ . Let us first arrange (60) in the form

$$\hat{U}_n \simeq \mathbb{1} - i\sqrt{\gamma}(\hat{A}\hat{b}_n^\dagger + \hat{A}^\dagger\hat{b}_n)\sqrt{\Delta t} - i\left(\hat{H}_{\text{vac}} - i\frac{\gamma}{2}(\hat{A}\hat{b}_n^\dagger + \hat{A}^\dagger\hat{b}_n)^2\right)\Delta t, \quad (91)$$

## IX. PHOTODETECTION AND QUANTUM TRAJECTORIES

As anticipated in the Introduction, a major advantage of collision models is that they naturally accommodate quantum weak measurements [17], which in the present quantum optics framework correspond to photodetection [54,70].

Let  $\{|k\rangle_n\}$  be an orthonormal basis of the  $n$ th time bin (henceforth we will mostly prefer the compact notation  $|k_n\rangle$ ). In the collisional picture, photodetection consists in measuring each time bin right after its collision with  $S$ . The photodetection scheme is defined by the measurement basis  $\{|k\rangle\}$ . Assuming an uncorrelated initial state of the time bins [cf. Eq. (66)], the (unnormalized) evolved state of the joint system after a specific sequence of measurement outcomes  $\{k_1, \dots, k_n\}$  is given by

where we used (16). Moreover, we allow the time-bin state  $|\chi_n\rangle$  to generally depend on  $\sqrt{\Delta t}$  (this is, for instance, the case of coherent states, as illustrated later). Hence, to lowest order, the expansion (31) holds. Note that the zeroth-order term was set equal to the time-bin vacuum state to ensure that the field energy density  $\langle \hat{b}_n^\dagger \hat{b}_n \rangle / \Delta t$  does not diverge in the limit  $\Delta t \rightarrow 0$ , which would lead to nonsensical photon-counting evolution [8,54] [we return to this issue shortly after Eq. (96)]. Also,  $|\chi_n^{(1)}\rangle$  and  $|\chi_n^{(2)}\rangle$  are subject to the constraints

$$\begin{aligned} \text{Re}\langle 0_n | \chi_n^{(1)} \rangle &= 0 \\ \langle \chi_n^{(1)} | \chi_n^{(1)} \rangle + 2\text{Re}\langle 0_n | \chi_n^{(2)} \rangle &= 0, \end{aligned} \quad (92)$$

which follow from the normalization condition of  $|\chi_n\rangle$  to the first order in  $\Delta t$ . Henceforth, the subscript  $n$  will be dropped in  $|0_n\rangle$ ,  $|\chi_n^{(1)}\rangle$ , and  $|\chi_n^{(2)}\rangle$ .

Plugging (91) and (31) into (87) and grouping together terms of the same order in  $\sqrt{\Delta t}$ , to leading order we get

$$\hat{K}_k = \langle k|0\rangle + \hat{K}_k^{(1)}\sqrt{\Delta t} + \hat{K}_k^{(2)}\Delta t, \quad (93)$$

where

$$\hat{K}_k^{(1)} = \langle k | \chi^{(1)} \rangle - i\sqrt{\gamma}\langle k|1\rangle\hat{A}, \quad (94)$$

$$\begin{aligned} \hat{K}_k^{(2)} &= \langle k | \chi^{(2)} \rangle - i\left[\sqrt{\gamma}\langle k|\hat{b}_n|\chi^{(1)}\rangle\hat{A}^\dagger + \langle k|\hat{b}_n^\dagger|\chi^{(1)}\rangle\hat{A}\right] \\ &+ \langle k|0\rangle\left(\hat{H}_{\text{vac}} - i\frac{\gamma}{2}\hat{A}^\dagger\hat{A}\right), \end{aligned} \quad (95)$$

with time-bin operators  $\hat{c}_\mu$  and emitter operators  $\hat{C}_\mu$  ( $\mu, \mu' = 1, 2$ ) given by (73). Replacing (93) into the conditional map (89) yields (to leading order)

$$\begin{aligned} \tilde{\rho}_n &= |\langle 0|k\rangle|^2 \rho_{n-1} + (\langle 0|k\rangle\hat{K}_k^{(2)}\rho_{n-1} + \text{H.c.})\Delta t \\ &+ \hat{K}_k^{(1)}\rho_{n-1}\hat{K}_k^{(1)\dagger}\Delta t. \end{aligned} \quad (96)$$

Summing the right-hand side over  $k$  (see Appendix C), we end up with the Lindblad master equation (32) [recall definition (20)], where the effective Hamiltonian  $\hat{H}_{\text{eff}}$  and jump

operators  $\hat{J}_k$  are given by (33) and (34), respectively (note that  $\hat{J}_k = \hat{K}_k^{(1)}$ ). This equation is equivalent to the (white-noise Gaussian) master equation (23) [or (28) for  $\gamma' = 0$ ], but at variance with this is not expressed in terms of field moments (requiring instead more detailed knowledge of the time-bin state). Thus,  $\hat{H}_{\text{eff}}$  and  $\hat{J}_k$  in fact define an unraveling of the master equation corresponding to a desired photodetection scheme. Two comments follow.

First, there are white-noise Gaussian field states, such as squeezed and thermal states, for which the zeroth-order term of expansion (31) differs from  $|0_n\rangle$  since their infinite bandwidth corresponds to an infinite photon flux (see also Ref. [8]). Equations (32)–(34) thus do not apply to such states.

Second, for most physically relevant field states, in a single time bin the single-photon and two-photon amplitudes are at most of order  $\sqrt{\Delta t}$  and  $\Delta t$ , respectively. This means that only the outcomes  $k = 0$  and  $k = 1$  occur with meaningful probability, corresponding to “click” and “no-click” outcomes, respectively (in line with most treatments of photodetection, which indeed limit themselves to click/no-click outcomes at each elementary time interval  $\Delta t$ ). Assuming a detector with perfect efficiency, the probability of a click in the time window  $[t_{n-1}, t_n]$  can be worked out from Eq. (90) for  $k = 1$  with the help of (92) and retaining only terms up to first order in  $\Delta t$  (see Appendix D). This yields the detection probability rate

$$\frac{p_1}{\Delta t} = |\langle \chi^{(1)} | 1 \rangle|^2 + (i\sqrt{\gamma} \langle 1 | \chi^{(1)} \rangle \langle \hat{A}^\dagger \rangle + \text{c.c.}) + \gamma \langle \hat{A}^\dagger \hat{A} \rangle. \quad (97)$$

When the field is in the vacuum state, this reduces to  $p_1/\Delta t = \gamma \langle \hat{A}^\dagger \hat{A} \rangle$ .

As an illustration, in the next section we will show how the above applies to photon counting in the case of a coherent-state wave packet. In the most general case of a mixed time-bin initial state, whose spectral decomposition reads  $\eta_n = \sum_\kappa q_\kappa |\chi_\kappa\rangle_n \langle \chi_\kappa|$  (with probabilities  $q_\kappa$  fulfilling  $\sum_\kappa q_\kappa = 1$ ), the Kraus operators will be indexed not only by the measurement outcome but also by the eigenstate  $|\chi_\kappa\rangle$ ,

$$\hat{K}_{k,\kappa} = \sqrt{q_\kappa} \langle k | \hat{U} | \chi_\kappa \rangle, \quad (98)$$

and (89) turns into a sum over  $\kappa$ ,

$$\tilde{\rho}_n = \sum_\kappa \hat{K}_{k,\kappa} \rho_{n-1} \hat{K}_{k,\kappa}^\dagger. \quad (99)$$

### A. Photon counting for a coherent-state wave packet

In the case of photon counting, the time-bin measurement basis are the Fock states  $\{|k_n\rangle\}$  with  $k = 0, 1, \dots$ . As anticipated in Sec. III C, a coherent-state wave packet in terms of time modes (4) reads [71]

$$|\xi\rangle = \exp\left(\int dt (\xi_t \hat{b}_t^\dagger - \xi_t^* \hat{b}_t)\right) |0\rangle, \quad (100)$$

with  $\xi_t$  the wave-packet amplitude in the time domain.<sup>1</sup> One can decompose the time integrals into a sum over intervals  $\{[t_{n-1}, t_n]\}$  and, if  $\Delta t$  is small enough, in each interval replace

$\xi_t \rightarrow \xi_n = \frac{1}{\Delta t} \int_{t_{n-1}}^{t_n} dt \xi_t$ . This yields

$$|\xi_n\rangle \simeq \exp\left(\sum_n (\xi_n \sqrt{\Delta t} \hat{b}_n^\dagger - \xi_n^* \sqrt{\Delta t} \hat{b}_n)\right) |0_n\rangle; \quad (101)$$

hence (66) holds for  $\eta_n = |\chi_n\rangle \langle \chi_n|$ . Here each  $|\chi_n\rangle$  [cf. Eq. (35)] is a single-mode coherent state of the  $n$ th time bin with amplitude  $\xi_n \sqrt{\Delta t}$ .<sup>4</sup> Expanding  $|\xi_n\rangle$  in powers of  $\sqrt{\Delta t}$ , one ends up with the effective Hamiltonian and jump operator in Eq. (36). Note that, in addition to  $\hat{H}_{\text{vac}}$ ,  $\hat{H}_{\text{eff}}$  features the standard drive Hamiltonian, arising from the first-order term  $\hat{V}_n$  in the collision unitary (60).<sup>5</sup> Also, note the  $c$ -number shift in  $\hat{J}_1$ . Analogous shifted jump operators, physically due to the coherent superposition of light emitted from  $S$  and the incoming beam, were previously derived (for normal emitters) via the input-output formalism (see, e.g., Refs. [54,55,72,73]). Finally, the photocounting rate (97) in this case is given by

$$\frac{dp_1}{dt} = |\xi_t|^2 - 2\sqrt{\gamma} \text{Im}(\xi_t \langle \hat{A}^\dagger \rangle) + \gamma \langle \hat{A}^\dagger \hat{A} \rangle, \quad (102)$$

where we used  $|\chi_n^{(1)}\rangle = \xi_n |1_n\rangle$  and passed to the continuous-time limit.

### B. Bidirectional field

If  $|\chi_n\rangle$  ( $|\chi_n'\rangle$ ) denotes the initial state of the right-going (left-going time bin) [recall Sec. VIII], Eq. (31) is generalized as

$$|\chi, \chi'\rangle = |0, 0\rangle + (|0, \chi'^{(1)}\rangle + |\chi^{(1)}, 0\rangle) \sqrt{\Delta t} \\ + (|0, \chi'^{(2)}\rangle + |\chi^{(2)}, 0\rangle + |\chi^{(1)}, \chi'^{(1)}\rangle) \Delta t \quad (103)$$

(we adopt the compact notation  $|a, b'\rangle = |a\rangle \otimes |b'\rangle$ ). Plugging (26) in Eq. (60), the collision unitary to the lowest order reads [cf. Eq. (91)]

$$\hat{U}_n \simeq \mathbb{1} - i(\sqrt{\gamma} \hat{A} \hat{b}_n^\dagger + \sqrt{\gamma'} \hat{A}' \hat{b}'_n^\dagger + \text{H.c.}) \sqrt{\Delta t} \\ - i\left(\hat{H}_{\text{vac}} - \frac{i}{2}(\sqrt{\gamma} \hat{A} \hat{b}_n^\dagger + \sqrt{\gamma'} \hat{A}' \hat{b}'_n^\dagger + \text{H.c.})^2\right) \Delta t, \quad (104)$$

with  $\hat{H}_{\text{vac}}$  given by Eq. (25).

A photodetection event now corresponds to a measurement of both the right- and left-going time bins in a basis  $|k, k'\rangle$  with  $\{|k\rangle\}$  ( $\{|k'\rangle\}$ ) an orthonormal basis of the right-going (left-going) time bin. The generalization of the expansion (93) can be worked out like in the unidirectional case; its explicit expression is reported in Appendix C. Finally, a procedure analogous to that leading to Eqs. (33) and (34) yields Eqs. (38) and (39) (see Appendix C for details).

## X. CONCLUSION

In this paper we formulated a collision-model-based description of quantum optics dynamics in the presence of many

<sup>4</sup>This procedure is somewhat heuristic, although physically intuitive. More rigorously, one replaces  $\hat{b}_t$  with (61) and next trace off all time-bin modes  $\hat{b}_{n,k \neq 0}$ . One can check that, in the limit  $\Delta t \rightarrow 0$ , each mode  $\hat{b}_{n,k \neq 0}$  reduces to the respective vacuum state [cf. Eq. (63)].

<sup>5</sup>Note that the  $1/\sqrt{\Delta t}$  factor in the coupling strength of  $\hat{V}_n$  cancels with the  $\sqrt{\Delta t}$  factor appearing in the amplitude of (35).

quantum emitters, each able to interact with a generally chiral field at many coupling points. The collisional picture maps the field into a stream of discrete time-bin modes interacting with the emitters in a conveyor-belt-like fashion. In the regime of negligible time delays (usual in most experiments) the dynamics is effectively represented as a sequence of pairwise collisions, each between a field time bin and all the emitters collectively. These at once undergo an internal dynamics ruled by an effective second-order Hamiltonian describing dipole-dipole interactions. This Hamiltonian originates from the fact that the traveling time bin reaches the system's coupling points in sequence, no matter how short the delays. As such, the effective Hamiltonian depends on the coupling point topology. We applied the collisional picture to derive a general Lindblad master equation of a set of (generally) giant emitters coupled to a chiral waveguide for an arbitrary white-noise Gaussian state of the field. This combines into a single equation and extends a variety of master equations used in quantum optics and waveguide QED. In addition, building on previous work [8], we worked out a general recipe that, for a given photodetection scheme, returns the effective Hamiltonian and jump operators generating the ensuing quantum trajectories.

For the sake of argument and in order to keep the number of parameters at a reasonable level, throughout we considered identical quantum emitters, each featuring a single transition coupled to the field and no external drive. Extending the theory so as to relax these assumptions is straightforward.

It is natural to compare the collision-model picture with the longstanding input-output formalism (IOF) of quantum optics (and methodologies underpinned by the latter such as the SLH approach [52]). As anticipated, these are both grounded on the same microscopic model, in particular the white-noise coupling assumption, and share the field representation in term of temporal modes. On the other hand, some significant differences stand out. One that is especially evident is that in the IOF time is a continuous variable, while in the collisional picture one in fact works with a discrete (coarse-grained) dynamics taking the continuous-time limit only at the end.

Notably, while in the IOF one evolves the operators in a Heisenberg-picture-like fashion, the collisional framework essentially deals with the evolution of states in the spirit of the Schrödinger picture. The role of input and output field operators in the IOF is played by the initial and final states of the time bins  $\eta_n$  and  $\eta'_n$ , while the central equation of the IOF that connects the output field to the input field and system operator is replaced by the pairwise unitary  $\hat{U}_n$  describing each collision. The collision unitary concept makes the collisional picture particularly advantageous to carry out tasks such as deriving in a natural way CPTP master equations, jump operators, or effective decoherence-free Hamiltonians [62]. Moreover, the joint emitter-field dynamics is in fact mapped into an effective quantum circuit, which can help quantum simulations and allows one to potentially take advantage of already developed quantum information/computing techniques. In this respect, it was recently proved [8] that all quantum optics master equations and photon detection schemes for a single (normal) emitter can be simulated through a collision model with time bins replaced by qubits. The present work in fact extends the same property to many giant emitters.

Finally, although in this paper the illustrations of the general theory mostly targeted the open dynamics of the emitters, we stress that the collisional picture captures the joint dynamics including the field. The framework is thus potentially as useful in problems such as multiphoton scattering from atoms [14] or nonequilibrium thermodynamics of quantum optics systems (or generally bosonic baths) [74].

## ACKNOWLEDGMENTS

We acknowledge support from MIUR through project PRIN (Project No. 2017SRN-BRK QUSHIP), the Canada First Research Excellence Fund, and NSERC. A.C. acknowledges support from the Government of the Russian Federation through Agreement No. 074-02-2018-330(2).

## APPENDIX A: DERIVATION OF THE MICROSCOPIC HAMILTONIAN

For completeness, here we report the derivation of the Hamiltonian (1), with  $\hat{H}_S$ ,  $\hat{H}_f$ , and  $\hat{V}$  given by Eqs. (2), (9), and (10), respectively, through linearization of the field dispersion law (see also, e.g., Ref. [75]).

Consider a one-dimensional bosonic field with normal-mode ladder operators  $\hat{a}_k$  and  $\hat{a}_k^\dagger$  where  $k$  is a (continuous) wave vector that can take both positive and negative values. Let  $\omega_k$  with  $\omega_k = \omega_{-k}$  be the dispersion law (for simplicity, we consider time-reversal invariant fields, but a more general treatment is possible). The free-field Hamiltonian can be written as

$$\hat{H}_f = \int_{-\infty}^0 dk \omega_k \hat{a}_k^\dagger \hat{a}_k + \int_0^{\infty} dk \omega_k \hat{a}_k^\dagger \hat{a}_k. \quad (\text{A1})$$

The field weakly and nonlocally couples to  $N_e$  quantum emitters, the  $\ell$ th coupling point of the  $j$ th emitter lying at position  $x_{j\ell}$ . The interaction Hamiltonian reads

$$\hat{V} = \sum_{j=1}^{N_e} \sum_{\ell=1}^{N_j} \hat{V}_{j\ell}, \quad (\text{A2})$$

with

$$\begin{aligned} \hat{V}_{j\ell} = & \hat{A}_j^\dagger \int_0^{\infty} dk \frac{g_k}{\sqrt{2\pi}} e^{ikx_{j\ell}} \hat{a}_k \\ & + \hat{A}_j^\dagger \int_{-\infty}^0 dk \frac{g_k}{\sqrt{2\pi}} e^{ikx_{j\ell}} \hat{a}_k + \text{H.c.}, \end{aligned} \quad (\text{A3})$$

where  $g_k$  is the coupling rate with mode  $k$ . The free Hamiltonian of the emitters  $\hat{H}_S$  is given in Eq. (2). In Eqs. (A1) and (A3), we conveniently split each integral into a positive and a negative  $k$  contribution in a way that, once right- and left-going modes are introduced as  $\hat{b}_k = \hat{a}_{k \geq 0}$  and  $\hat{b}'_k = \hat{a}_{k < 0}$ , the free-field and interaction Hamiltonian can be expressed as

$$\hat{H}_f = \int_{-\infty}^0 dk \omega_k \hat{b}'_k \hat{b}'_k + \int_0^{\infty} dk \omega_k \hat{b}_k \hat{b}_k, \quad (\text{A4})$$

$$\begin{aligned} \hat{V}_{j\ell} = & \hat{A}_j^\dagger \int_0^{\infty} dk \frac{g_k}{\sqrt{2\pi}} e^{ikx_{j\ell}} \hat{b}_k \\ & + \hat{A}_j^\dagger \int_{-\infty}^0 dk \frac{g_k}{\sqrt{2\pi}} e^{ikx_{j\ell}} \hat{b}'_k + \text{H.c.} \end{aligned} \quad (\text{A5})$$

Since the coupling is weak, the emitters significantly interact only with a narrow field's bandwidth centered at the emitter frequency  $\omega_0 = \omega_{k_0} = \omega_{-k_0}$ . Accordingly, the dispersion law and coupling rates are approximated as

$$\omega_{k \geq 0} \simeq \omega_0 + v(k - k_0), \quad \omega_{k < 0} \simeq \omega_0 - v(k + k_0), \quad (\text{A6})$$

$$g_{k \geq 0} \simeq g_{k_0} = g, \quad g_{k < 0} \simeq g_{-k_0} = g', \quad (\text{A7})$$

with  $v = \partial_k \omega_k$  the field's group velocity. At the same time, the limits of integration in each integral in Eqs. (A4) and (A5) can be extended to the entire real axis. Thereby, (A4) and (A5) are turned into

$$\begin{aligned} \hat{H}_f &= \omega_0 \int_{-\infty}^{\infty} dk (\hat{b}_k^\dagger \hat{b}_k + \hat{b}_k'^\dagger \hat{b}_k') \\ &+ \int_{-\infty}^{\infty} dk v(k - k_0) \hat{b}_k^\dagger \hat{b}_k - \int_{-\infty}^{\infty} dk v(k + k_0) \hat{b}_k'^\dagger \hat{b}_k', \end{aligned} \quad (\text{A8})$$

$$\begin{aligned} \hat{V}_{j\ell} &= \hat{A}_j^\dagger e^{ik_0 x_{j\ell}} \int_{-\infty}^{\infty} dk \frac{g}{\sqrt{2\pi}} e^{i(k-k_0)x_{j\ell}} \hat{b}_k \\ &+ \hat{A}_j^\dagger e^{-ik_0 x_{j\ell}} \int_{-\infty}^{\infty} dk \frac{g'}{\sqrt{2\pi}} e^{i(k+k_0)x_{j\ell}} \hat{b}_k' + \text{H.c.} \end{aligned} \quad (\text{A9})$$

Note the appearance of phase factors  $e^{\pm ik_0 x_{j\ell}}$ . Next, by making the variable change  $k - k_0 \rightarrow k$  in integrals featuring  $\hat{b}_k$ 's and  $-(k + k_0) \rightarrow k$  in integrals featuring  $\hat{b}_k'$ 's, we get

$$\begin{aligned} \hat{H}_f &= \omega_0 \int_{-\infty}^{\infty} dk (\hat{b}_k^\dagger \hat{b}_k + \hat{b}_k'^\dagger \hat{b}_k') \\ &+ \int_{-\infty}^{\infty} dk vk \hat{b}_k^\dagger \hat{b}_k + \int_{-\infty}^{\infty} dk vk \hat{b}_k'^\dagger \hat{b}_k', \end{aligned} \quad (\text{A10})$$

$$\begin{aligned} \hat{V}_{j\ell} &= \hat{A}_j^\dagger e^{ik_0 x_{j\ell}} \int_{-\infty}^{\infty} dk \frac{g}{\sqrt{2\pi}} e^{ikx_{j\ell}} \hat{b}_k \\ &+ \hat{A}_j^\dagger e^{-ik_0 x_{j\ell}} \int_{-\infty}^{\infty} dk \frac{g'}{\sqrt{2\pi}} e^{-ikx_{j\ell}} \hat{b}_k' + \text{H.c.}, \end{aligned} \quad (\text{A11})$$

where we redefined the field operators as  $\hat{b}_{k+k_0} \rightarrow \hat{b}_k$  and  $\hat{b}'_{-(k+k_0)} \rightarrow \hat{b}'_k$ . Finally, changing to the frequency domain  $\omega$ , we end up with

$$\begin{aligned} \hat{H}_f &= \int_{-\infty}^{\infty} d\omega \omega \hat{b}_\omega^\dagger \hat{b}_\omega + \int_{-\infty}^{\infty} d\omega \omega \hat{b}'_\omega{}^\dagger \hat{b}'_\omega, \quad (\text{A12}) \\ \hat{V}_{j\ell} &= \hat{A}_j^\dagger e^{i\omega_0 \tau_{j\ell}} \int_{-\infty}^{\infty} d\omega \sqrt{\frac{\gamma}{2\pi}} e^{i\omega \tau_{j\ell}} \hat{b}_\omega \end{aligned}$$

$$+ \hat{A}_j^\dagger e^{-i\omega_0 \tau_{j\ell}} \int_{-\infty}^{\infty} d\omega \sqrt{\frac{\gamma'}{2\pi}} e^{-i\omega \tau_{j\ell}} \hat{b}'_\omega + \text{H.c.}, \quad (\text{A13})$$

where  $\tau_{j\ell} = x_{j\ell}/v$ ,  $\hat{b}_\omega = \hat{b}_k/\sqrt{v}$ ,  $\hat{b}'_\omega = \hat{b}'_k/\sqrt{v}$ ,  $\gamma = g^2/v$ , and  $\gamma' = g'^2/v$ . Note the two equivalent ways to express the phase factors  $e^{\pm i\omega_0 \tau_{j\ell}} = e^{\pm ik_0 x_{j\ell}}$ .

## APPENDIX B: TERMS $\hat{\mathcal{H}}_{\text{th}}^{(1)}$ and $\hat{\mathcal{H}}_{\text{sq}}^{(1)}$

As anticipated in the main text, for  $\tau_v - \tau_{v-1} \ll \Delta t$  for all  $v$ 's (negligible time delays) and setting  $\tau_1 = 0$ , in Eqs. (54) and (55) all time delays can be neglected, replacing  $s - \tau_v$  ( $s' - \tau_{v'}$ ) with  $s$  ( $s'$ ). This yields

$$\hat{\mathcal{H}}_{\text{th}}^{(1)} \simeq \frac{i\gamma}{2\Delta t} \sum_{v,v'} [\hat{\mathcal{A}}_v, \hat{\mathcal{A}}_{v'}^\dagger] \int_{t_{n-1}}^{t_n} ds \int_{t_{n-1}}^{t_n} ds' \text{sgn}(s' - s) \hat{b}_s^\dagger \hat{b}_{s'}, \quad (\text{B1})$$

$$\begin{aligned} \hat{\mathcal{H}}_{\text{sq}}^{(1)} &\simeq \frac{i\gamma}{4\Delta t} \sum_{v,v'} [\hat{\mathcal{A}}_v, \hat{\mathcal{A}}_{v'}] \int_{t_{n-1}}^{t_n} ds \int_{t_{n-1}}^{t_n} ds' \text{sgn}(s' - s) \hat{b}_s^\dagger \hat{b}_{s'}^\dagger \\ &+ \text{H.c.}, \end{aligned} \quad (\text{B2})$$

where we introduced the sign function to get more compact expressions. The integral in  $\hat{\mathcal{H}}_{\text{sq}}^{(1)}$  vanishes identically, due to the antisymmetry of the integrand under the exchange  $s \leftrightarrow s'$ . The same argument applies for a bidirectional field [cf. Eq. (80)], in which case the integrals in  $\hat{\mathcal{H}}_{\text{sq}}^{(1)}$  feature extra terms with the same symmetry.

To evaluate  $\hat{\mathcal{H}}_{\text{th}}^{(1)}$ , we expand the field  $\hat{b}_t$  in terms of time-bin modes  $\hat{b}_{n,k}$  [cf. Eqs. (61) and (62)]. This yields

$$\hat{H}_{\text{th}} = -\gamma \sum_{v,v'} [\hat{\mathcal{A}}_v, \hat{\mathcal{A}}_{v'}^\dagger] \sum_{k \neq 0} \frac{\hat{b}_{n,k}^\dagger \hat{b}_{n,k} - (\hat{b}_{n,k}^\dagger \hat{b}_{n,0} + \text{H.c.})}{2\pi k}. \quad (\text{B3})$$

As discussed in Sec. VB, for  $\Delta t$  short enough, each mode  $\hat{b}_{n,k \neq 0}$  is in its own vacuum state  $|0\rangle_{n,k}$  [cf. Eq. (63)]. Thus, effectively,  $\hat{H}_{\text{th}} = 0$ .

For a bidirectional field, we will additionally expand  $\hat{b}'_t$  in terms of left-going time-bin modes  $\hat{b}'_{n,k}$  [defined in full analogy with (62)]. This results in an expression similar to (B3), featuring overall terms of type  $\sim \hat{\beta}_{n,k}^\dagger \hat{\beta}_{n',k'}$  with  $\beta, \beta' = b, b'$  and where at least one of  $k$  and  $k'$  is nonzero. Thus  $\hat{\mathcal{H}}_{\text{th}}^{(1)}$  is negligible when modes  $b_{n,k \neq 0}$  and  $b'_{n,k \neq 0}$  are in the vacuum state.

## APPENDIX C: DERIVATION OF $\hat{H}_{\text{eff}}$ AND JUMP OPERATORS

Summing over  $k$ , the right-hand side of (96) yields the CPTP map  $\mathcal{E}[\rho_{n-1}] = \sum_k \hat{K}_k \rho_{n-1} \hat{K}_k^\dagger$ . Using (93), this can be arranged as

$$\mathcal{E}[\rho_{n-1}] = \rho_{n-1} + \sum_k (\langle k|0\rangle \rho_{n-1} \hat{K}_k^{(1)\dagger} + \text{H.c.}) \sqrt{\Delta t} + \sum_k (\langle k|0\rangle \rho_{n-1} \hat{K}_k^{(2)\dagger} + \text{H.c.} + \hat{K}_k^{(1)} \rho_{n-1} \hat{K}_k^{(1)\dagger}) \Delta t. \quad (\text{C1})$$

The contribution  $\sum_k (\dots) \sqrt{\Delta t}$  vanishes since we can arrange the sum as

$$\sum_k (\dots) = 2 \text{Re} \langle 0 | \chi_n^{(1)} \rho_{n-1} - i[\rho_{n-1}, \sqrt{\gamma} (\langle 0 | \hat{b}_n | 0 \rangle \hat{\mathcal{A}}^\dagger + \text{H.c.})]. \quad (\text{C2})$$

This is zero due to Eq. (92) and of course  $\langle 0 | \hat{b}_n | 0 \rangle = 0$ .

The remaining terms in (C1), using  $\Delta\rho_n = \mathcal{E}[\rho_{n-1}] - \rho_{n-1}$ , yield

$$\frac{\Delta\rho_n}{\Delta t} = \rho_{n-1}\hat{A}^\dagger + \hat{A}\rho_{n-1} + \sum_k \hat{J}_k \rho_{n-1} \hat{J}_k^\dagger, \quad (\text{C3})$$

where we defined

$$\hat{A} = \sum_k \langle 0|k\rangle \hat{K}_k^{(2)}, \quad \hat{J}_k = \hat{K}_k^{(1)}. \quad (\text{C4})$$

We can set  $\hat{A} = \hat{R} - i\hat{H}_{\text{eff}}$ , with  $\hat{R} = \frac{1}{2}(\hat{A} + \hat{A}^\dagger)$  and  $\hat{H}_{\text{eff}} = \frac{i}{2}(\hat{A} - \hat{A}^\dagger)$ . With this replacement, Eq. (C3) becomes

$$\frac{\Delta\rho_n}{\Delta t} = -i[\hat{H}_{\text{eff}}, \rho_{n-1}] + [\hat{R}, \rho_{n-1}]_+ + \sum_k \hat{J}_k \rho_{n-1} \hat{J}_k^\dagger. \quad (\text{C5})$$

Since the map  $\mathcal{E}$  is in particular trace preserving,  $\text{Tr}_S(\Delta\rho_n)$  always vanishes, that is,

$$\text{Tr}_S \left( [\hat{R}, \rho_{n-1}]_+ + \sum_k \hat{J}_k \rho_{n-1} \hat{J}_k^\dagger \right) = 0. \quad (\text{C6})$$

Since this must hold for any  $\rho_{n-1}$ , the argument of the trace is zero, yielding  $\hat{R} = -\frac{1}{2} \sum_k \hat{J}_k^\dagger \hat{J}_k$  [66]. Replacing back in (C5), we thus obtain the dissipator of Eq. (32). To work out  $\hat{H}_{\text{eff}}$ , we explicitly calculate  $\hat{A}$  [cf. Eq. (C4)] with the help of (73) and (95), obtaining

$$\hat{A} = \langle 0|\chi^{(2)}\rangle - i\sqrt{\gamma}\langle 1|\chi^{(1)}\rangle \hat{\mathcal{A}}^\dagger - i\hat{H}_{\text{vac}} - \frac{\gamma}{2} \hat{\mathcal{A}}^\dagger \hat{\mathcal{A}} \quad (\text{C7})$$

(note that the last term is Hermitian). Plugging this in  $\hat{H}_{\text{eff}} = \frac{i}{2}(\hat{A} - \hat{A}^\dagger)$  and neglecting an irrelevant constant term  $\text{Im}\langle 0|\chi^{(2)}\rangle$ , we end up with the effective Hamiltonian in Eq. (33), which concludes the proof.

#### Bidirectional field

Generalizing (87) as  $\hat{K}_{k,k'} = \langle k, k' | \hat{U}_n | \chi, \chi' \rangle$ , the low-order expansion of each Kraus operators reads [cf. Eq. (93)]

$$\hat{K}_{k,k'} = \hat{K}_{k,k'}^{(0)} + \hat{K}_{k,k'}^{(1)} \sqrt{\Delta t} + \hat{K}_{k,k'}^{(2)} \Delta t. \quad (\text{C8})$$

Using Eqs. (103) and (104) and defining left-going primed operators in full analogy with Eq. (72), we get

$$\hat{K}_{k,k'}^{(0)} = \langle k|0\rangle \langle k'|0\rangle, \quad (\text{C9})$$

$$\hat{K}_{k,k'}^{(1)} = \langle k|0\rangle \langle k'|\chi^{(1)}\rangle + \langle k|\chi^{(1)}\rangle \langle k'|0\rangle - i(\sqrt{\gamma}\langle k|1\rangle \langle k'|0\rangle \hat{\mathcal{A}} + \sqrt{\gamma'}\langle k|0\rangle \langle k'|1\rangle \hat{\mathcal{A}}'), \quad (\text{C10})$$

$$\begin{aligned} \hat{K}_{k,k'}^{(2)} = & \langle k|0\rangle \langle k'|\chi^{(2)}\rangle + \langle k'|0\rangle \langle k|\chi^{(2)}\rangle + \langle k|\chi^{(1)}\rangle \langle k'|\chi^{(1)}\rangle - i \left( \langle k|0\rangle \langle k'|0\rangle \hat{H}_{\text{vac}} - \frac{i}{2} (\gamma \langle k'|0\rangle \langle k|0\rangle \hat{\mathcal{A}}^\dagger \hat{\mathcal{A}} \right. \\ & \left. + \gamma' \langle k|0\rangle \langle k'|0\rangle \hat{\mathcal{A}}^\dagger \hat{\mathcal{A}}' + 2\sqrt{\gamma\gamma'} \langle k'|1\rangle \langle k|1\rangle \hat{\mathcal{A}}' \hat{\mathcal{A}} \right) - i(\sqrt{\gamma}[\langle k|1\rangle \langle k'|\chi^{(1)}\rangle + \langle k'|0\rangle \langle k|\hat{b}_n^\dagger|\chi^{(1)}\rangle] \hat{\mathcal{A}} \\ & + \langle k'|0\rangle \langle k|\hat{b}_n|\chi^{(1)}\rangle \hat{\mathcal{A}}^\dagger] + \sqrt{\gamma'}[\langle k'|1\rangle \langle k|\chi^{(1)}\rangle + \langle k|0\rangle \langle k'|\hat{b}_n^\dagger|\chi^{(1)}\rangle] \hat{\mathcal{A}}' + \langle k|0\rangle \langle k'|\hat{b}_n|\chi^{(1)}\rangle \hat{\mathcal{A}}^\dagger]). \end{aligned} \quad (\text{C11})$$

Plugging these into Eq. (C1) with the replacements  $|0\rangle \rightarrow |0, 0\rangle$  and  $k \rightarrow k, k'$  yields the CPTP map at each collision. Terms  $\sim\sqrt{\Delta t}$  vanish using an argument analogous to the unidirectional case. Essentially for the same reason, when summing over  $(k, k')$ , one finds that crossed terms  $\sim\hat{\mathcal{A}}'\hat{\mathcal{A}}$  in  $\hat{K}^{(2)}$  yield a zero contribution. Finally, repeating reasoning analogous to the unidirectional case leads to Eqs. (38) and (39).

#### APPENDIX D: DERIVATION OF EQ. (97)

From Eq. (93) we get to leading order

$$\hat{K}_k^\dagger \hat{K}_k = |\langle 0|k\rangle|^2 + (\langle 0|k\rangle \hat{K}_k^{(1)} + \langle k|0\rangle \hat{K}_k^{(1)\dagger}) \sqrt{\Delta t} + (\langle 0|k\rangle \hat{K}_k^{(2)} + \langle k|0\rangle \hat{K}_k^{(2)\dagger} + \hat{K}_k^{(1)\dagger} \hat{K}_k^{(1)}) \Delta t. \quad (\text{D1})$$

For  $k = 1$ , this reduces to  $\hat{K}_k^{(1)\dagger} \hat{K}_k^{(1)} \Delta t$ . Applying Eq. (94) and dividing by  $\Delta t$ , we end up with Eq. (97). Analogously for the bidirectional field, since  $\hat{K}_{1,0}^{(0)} = \hat{K}_{0,1}^{(0)} = 0$ , the only contributing term is  $\hat{K}_{0,1}^{(1)\dagger} \hat{K}_{0,1}^{(1)} + \hat{K}_{1,0}^{(1)\dagger} \hat{K}_{1,0}^{(1)}$ , then

$$\frac{P_1}{\Delta t} = |\langle \chi^{(1)}|1\rangle|^2 + (i\sqrt{\gamma}\langle 1|\chi^{(1)}\rangle \langle \hat{\mathcal{A}}^\dagger + \text{c.c.}) + \gamma \langle \hat{\mathcal{A}}^\dagger \hat{\mathcal{A}} | \langle \chi^{(1)}|1\rangle|^2 + (i\sqrt{\gamma'}\langle 1|\chi^{(1)}\rangle \langle \hat{\mathcal{A}}^\dagger + \text{c.c.}) + \gamma' \langle \hat{\mathcal{A}}^\dagger \hat{\mathcal{A}} \rangle. \quad (\text{D2})$$

- [1] H. Pichler and P. Zoller, Photonic Circuits with Time Delays and Quantum Feedback, *Phys. Rev. Lett.* **116**, 093601 (2016).
- [2] A. L. Grimsmo, Time-Delayed Quantum Feedback Control, *Phys. Rev. Lett.* **115**, 060402 (2015).
- [3] S. J. Whalen, A. L. Grimsmo, and H. J. Carmichael, Open quantum systems with delayed coherent feedback, *Quantum Sci. Technol.* **2**, 044008 (2017).
- [4] F. Ciccarello, Collision models in quantum optics, *Quantum Meas. Quantum Metrol.* **4**, 53 (2017).
- [5] D. Cilluffo and F. Ciccarello, in *Advances in Open Systems and Fundamental Tests of Quantum Mechanics*, edited by B. Vacchini, H.-P. Breuer, and A. Bassi, Springer Proceedings in Physics Vol. 237 (Springer, Berlin, 2019), pp. 29–40.
- [6] K. A. Fischer, R. Trivedi, V. Ramasesh, I. Siddiqi, and J. Vučković, Scattering into one-dimensional waveguides from a coherently-driven quantum-optical system, *Quantum* **2**, 69 (2018).
- [7] K. Fischer, Derivation of the quantum-optical master equation based on coarse-graining of time, *J. Phys. Commun.* **2**, 091001 (2018).
- [8] J. A. Gross, C. M. Caves, G. J. Milburn, and J. Combes, Qubit models of weak continuous measurements: Markovian conditional and open-system dynamics, *Quantum Sci. Technol.* **3**, 024005 (2018).
- [9] S. J. Whalen, Collision model for non-Markovian quantum trajectories, *Phys. Rev. A* **100**, 052113 (2019).
- [10] A. Dabrowska, G. Sarbicki, and D. Chruscinski, Quantum trajectories for a system interacting with environment in a single-photon state: Counting and diffusive processes, *Phys. Rev. A* **96**, 053819 (2017).
- [11] G. Vissers and L. Bouten, Implementing quantum stochastic differential equations on a quantum computer, *Quantum Inf. Process.* **18**, 152 (2019).
- [12] A. Dabrowska, G. Sarbicki, and D. Chruscinski, Quantum trajectories for a system interacting with environment in  $N$ -photon state, *J. Phys. A: Math. Theor.* **52**, 105303 (2019).
- [13] A. M. Dabrowska, From *a posteriori* to *a priori* solutions for a two-level system interacting with a single-photon wavepacket, *J. Opt. Soc. Am. B* **37**, 1240 (2020).
- [14] M. Heuck, K. Jacobs, and D. R. Englund, Photon-photon interactions in dynamically coupled cavities, *Phys. Rev. A* **101**, 042322 (2020).
- [15] M. Heuck, K. Jacobs, and D. R. Englund, Controlled-Phase Gate using Dynamically Coupled Cavities and Optical Nonlinearities, *Phys. Rev. Lett.* **124**, 160501 (2020).
- [16] C. M. Caves and G. J. Milburn, Quantum-mechanical model for continuous position measurements, *Phys. Rev. A* **36**, 5543 (1987).
- [17] T. A. Brun, A simple model of quantum trajectories, *Am. J. Phys.* **70**, 719 (2002).
- [18] V. Giovannetti and G. M. Palma, Master Equations for Correlated Quantum Channels, *Phys. Rev. Lett.* **108**, 040401 (2012).
- [19] T. Rybár, S. N. Filippov, M. Ziman, and V. Bužek, Simulation of indivisible qubit channels in collision models, *J. Phys. B* **45**, 154006 (2012).
- [20] F. Ciccarello, G. M. Palma, and V. Giovannetti, Collision-model-based approach to non-Markovian quantum dynamics, *Phys. Rev. A* **87**, 040103(R) (2013).
- [21] N. K. Bernardes, A. R. R. Carvalho, C. H. Monken, and M. F. Santos, Environmental correlations and Markovian to non-Markovian transitions in collisional models, *Phys. Rev. A* **90**, 032111 (2014).
- [22] R. McCloskey and M. Paternostro, Non-Markovianity and system-environment correlations in a microscopic collision model, *Phys. Rev. A* **89**, 052120 (2014).
- [23] J. Jin, V. Giovannetti, R. Fazio, F. Sciarrino, P. Mataloni, A. Crespi, and R. Osellame, All-optical non-Markovian stroboscopic quantum simulator, *Phys. Rev. A* **91**, 012122 (2015).
- [24] S. Kretschmer, K. Luoma, and W. T. Strunz, Collision model for non-Markovian quantum dynamics, *Phys. Rev. A* **94**, 012106 (2016).
- [25] S. Lorenzo, F. Ciccarello, and G. M. Palma, Class of exact memory-kernel master equations, *Phys. Rev. A* **93**, 052111 (2016).
- [26] S. Lorenzo, F. Ciccarello, and G. M. Palma, Composite quantum collision models, *Phys. Rev. A* **96**, 032107 (2017).
- [27] S. N. Filippov, J. Piilo, S. Maniscalco, and M. Ziman, Divisibility of quantum dynamical maps and collision models, *Phys. Rev. A* **96**, 032111 (2017).
- [28] S. Campbell, F. Ciccarello, G. M. Palma, and B. Vacchini, System-environment correlations and Markovian embedding of quantum non-Markovian dynamics, *Phys. Rev. A* **98**, 012142 (2018).
- [29] V. Scarani, M. Ziman, P. Štelmachovič, N. Gisin, and V. Bužek, Thermalizing Quantum Machines: Dissipation and Entanglement, *Phys. Rev. Lett.* **88**, 097905 (2002).
- [30] D. Karevski and T. Platini, Quantum Nonequilibrium Steady States Induced by Repeated Interactions, *Phys. Rev. Lett.* **102**, 207207 (2009).
- [31] R. Uzdin and R. Kosloff, The multilevel four-stroke swap engine and its environment, *New J. Phys.* **16**, 095003 (2014).
- [32] S. Lorenzo, R. McCloskey, F. Ciccarello, M. Paternostro, and G. M. Palma, Landauer's Principle in Multipartite Open Quantum System Dynamics, *Phys. Rev. Lett.* **115**, 120403 (2015).
- [33] P. Strasberg, G. Schaller, T. Brandes, and M. Esposito, Quantum and Information Thermodynamics: A Unifying Framework Based on Repeated Interactions, *Phys. Rev. X* **7**, 021003 (2017).
- [34] G. De Chiara, G. Landi, A. Hewgill, B. Reid, A. Ferraro, A. J. Roncaglia, and M. Antezza, Reconciliation of quantum local master equations with thermodynamics, *New J. Phys.* **20**, 113024 (2018).
- [35] D. Kafri and J. M. Taylor, A noise inequality for classical forces, [arXiv:1311.4558](https://arxiv.org/abs/1311.4558).
- [36] N. Altamirano, P. Corona-Ugalde, R. B. Mann, and M. Zych, Unitarity, feedback, interactions—Dynamics emergent from repeated measurements, *New J. Phys.* **19**, 013035 (2017).
- [37] U. Schollwöck, The density-matrix renormalization group in the age of matrix product states, *Ann. Phys. (NY)* **326**, 96 (2011).
- [38] S. Mahmoodian, G. Calajó, D. E. Chang, K. Hammerer, and A. S. Sørensen, Dynamics of Many-Body Photon Bound States in Chiral Waveguide QED, *Phys. Rev. X* **10**, 031011 (2020).
- [39] P.-O. Guimond, B. Vermersch, M. L. Juan, A. Sharafiev, G. Kirchmair, and P. Zoller, A unidirectional on-chip photonic interface for superconducting circuits, *npj Quantum Inf.* **6**, 32 (2020).
- [40] X. Gu, A. F. Kockum, A. Miranowicz, Y.-x. Liu, and F. Nori, Microwave photonics with superconducting quantum circuits, *Phys. Rep.* **718–719**, 1 (2017).

- [41] A. F. Kockum, Quantum optics with giant atoms—The first five years, [arXiv:1912.13012](https://arxiv.org/abs/1912.13012).
- [42] M. V. Gustafsson, T. Aref, A. F. Kockum, M. K. Ekström, G. Johansson, and P. Delsing, Propagating phonons coupled to an artificial atom, *Science* **346**, 207 (2014).
- [43] B. Kannan, M. Ruckriegel, D. Campbell, A. F. Kockum, J. Braumüller, D. Kim, M. Kjaergaard, P. Krantz, A. Melville, B. M. Niedzielski *et al.*, Waveguide quantum electrodynamics with giant superconducting artificial atoms, *Nature (London)* **583**, 775 (2020).
- [44] M. Aspelmeyer, T. J. Kippenberg, and F. Marquardt, Cavity optomechanics, *Rev. Mod. Phys.* **86**, 1391 (2014).
- [45] K. Hammerer, A. S. Sørensen, and E. S. Polzik, Quantum interface between light and atomic ensembles, *Rev. Mod. Phys.* **82**, 1041 (2010).
- [46] T. M. Karg, B. Gouraud, P. Treutlein, and K. Hammerer, Remote Hamiltonian interactions mediated by light, *Phys. Rev. A* **99**, 063829 (2019).
- [47] C. W. Gardiner and P. Zoller, *Quantum Noise: A Handbook of Markovian and Non-Markovian Quantum Stochastic Methods with Applications to Quantum Optics* (Springer Science + Business Media, New York, 2004).
- [48] T. Shi, D. E. Chang, and J. I. Cirac, Multiphoton-scattering theory and generalized master equations, *Phys. Rev. A* **92**, 053834 (2015).
- [49] D. Roy, C. M. Wilson, and O. Firstenberg, Colloquium: Strongly interacting photons in one-dimensional continuum, *Rev. Mod. Phys.* **89**, 021001 (2017).
- [50] Z. Liao, X. Zeng, H. Nha, and M. S. Zubairy, Photon transport in a one-dimensional nanophotonic waveguide QED system, *Phys. Scr.* **91**, 063004 (2016).
- [51] A. F. Kockum, G. Johansson, and F. Nori, Decoherence-Free Interaction between Giant Atoms in Waveguide Quantum Electrodynamics, *Phys. Rev. Lett.* **120**, 140404 (2018).
- [52] J. Combes, J. Kerckhoff, and M. Sarovar, The SLH framework for modeling quantum input-output networks, *Adv. Phys.: X* **2**, 784 (2017).
- [53] P. Lodahl, S. Mahmoodian, S. Stobbe, A. Rauschenbeutel, P. Schneeweiss, J. Volz, H. Pichler, and P. Zoller, Chiral quantum optics, *Nature (London)* **541**, 473 (2017).
- [54] H. M. Wiseman and G. J. Milburn, *Quantum Measurement and Control* (Cambridge University Press, Cambridge, 2009).
- [55] M. T. Manzoni, D. E. Chang, and J. S. Douglas, Simulating quantum light propagation through atomic ensembles using matrix product states, *Nat. Commun.* **8**, 1743 (2017).
- [56] C. W. Gardiner, Driving a Quantum System with the Output Field from Another Driven Quantum System, *Phys. Rev. Lett.* **70**, 2269 (1993).
- [57] H. J. Carmichael, Quantum Trajectory Theory for Cascaded Open Systems, *Phys. Rev. Lett.* **70**, 2273 (1993).
- [58] J. You, Z. Liao, S.-W. Li, and M. S. Zubairy, Waveguide quantum electrodynamics in squeezed vacuum, *Phys. Rev. A* **97**, 023810 (2018).
- [59] A. Gonzalez-Tudela, D. Martin-Cano, E. Moreno, L. Martin-Moreno, C. Tejedor, and F. J. Garcia-Vidal, Entanglement of Two Qubits Mediated by One-Dimensional Plasmonic Waveguides, *Phys. Rev. Lett.* **106**, 020501 (2011).
- [60] D. E. Chang, L. Jiang, A. V. Gorshkov, and H. J. Kimble, Cavity QED with atomic mirrors, *New J. Phys.* **14**, 063003 (2012).
- [61] T. Tufarelli, F. Ciccarello, and M. S. Kim, Dynamics of spontaneous emission in a single-end photonic waveguide, *Phys. Rev. A* **87**, 013820 (2013).
- [62] A. Carollo, D. Cilluffo, and F. Ciccarello, Mechanism of decoherence-free coupling between giant atoms, [arXiv:2006.13940](https://arxiv.org/abs/2006.13940) [quant-ph] (2020).
- [63] K. M. Gheri, K. Ellinger, T. Pellizzari, and P. Zoller, Photon-wavepackets as flying quantum bits, in *Quantum Computing*, edited by S. L. Braunstein (Wiley-VCH, Verlag GmbH & Co. KGaA, 2005), Chap. 5, pp. 95–109.
- [64] K. Lalumière, B. C. Sanders, A. F. van Loo, A. Fedorov, A. Wallraff, and A. Blais, Input-output theory for waveguide QED with an ensemble of inhomogeneous atoms, *Phys. Rev. A* **88**, 043806 (2013).
- [65] W. Magnus, On the exponential solution of differential equations for a linear operator, *Commun. Pure Appl. Math.* **7**, 649 (1954).
- [66] H.-P. Breuer and F. Petruccione, *The Theory of Open Quantum Systems* (Oxford University Press, Oxford, 2007).
- [67] Y.-L. L. Fang, F. Ciccarello, and H. U. Baranger, Non-Markovian dynamics of a qubit due to single-photon scattering in a waveguide, *New J. Phys.* **20**, 043035 (2018).
- [68] H. Pichler, T. Ramos, A. J. Daley, and P. Zoller, Quantum optics of chiral spin networks, *Phys. Rev. A* **91**, 042116 (2015).
- [69] P.-O. Guimond, M. Pletyukhov, H. Pichler, and P. Zoller, Delayed coherent quantum feedback from a scattering theory and a matrix product state perspective, *Quantum Sci. Technol.* **2**, 044012 (2017).
- [70] H. Carmichael, *An Open Systems Approach to Quantum Optics*, Lecture Notes in Physics Monographs, Vol. 18 (Springer-Verlag, Berlin, 1993).
- [71] R. Loudon, *The Quantum Theory of Light* (OUP, Oxford, 2000).
- [72] X. H. H. Zhang and H. U. Baranger, Quantum interference and complex photon statistics in waveguide QED, *Phys. Rev. A* **97**, 023813 (2018).
- [73] D. Cilluffo, S. Lorenzo, G. M. Palma, and F. Ciccarello, Quantum jump statistics with a shifted jump operator in a chiral waveguide, *J. Stat. Mech.* (2019) 104004.
- [74] C. Elouard, D. Herrera-Martí, M. Esposito, and A. Auffèves, Thermodynamics of optical Bloch equations, *New J. Phys.* (2020), doi: 10.1088/1367-2630/abbd6e.
- [75] J. T. Shen and S. Fan, Theory of single-photon transport in a single-mode waveguide. I. Coupling to a cavity containing a two-level atom, *Phys. Rev. A* **79**, 023837 (2009).